Z. Phys. C - Particles and Fields 29, 459–475 (1985)

Zeitschrift für Physik C Particles and Fields

Large p_T Double Photon Production in Hadronic Collisions— Beyond Leading Logarithm QCD Calculation

P. Aurenche, A. Douiri
LAPP, F-74019 Annecy-Le-Vieux, France

R. Baier
Fakultät für Physik, Universität Bielefeld, 4800 Bielefeld 1, Federal Republic of Germany

M. Fontannaz, D. Schiff
Laboratoire de Physique Théorique et Hautes Energies,[1] Bâtiment 211, Université Paris-Sud, F-91405 Orsay, France

Received 3 June 1985

Abstract. We calculate $O(\alpha_s)$ corrections to large p_T double photon production in hadronic collisions. We find that these corrections to the basic $q\bar{q}\to\gamma\gamma$ subprocess are important, preventing to describe double photon production on the basis of the leading logarithm approximation only. We give a phenomenological discussion of the results obtained at SPS, ISR and Sp$\bar{p}$S energies. In particular, we investigate how the effect of the intrinsic parton $\langle\kappa_T\rangle$ may be disentangled from the perturbative contribution. We also calculate the aplanarity distribution characteristic of 3 jet events.

I. Introduction

Prompt γ production in hadronic collisions has been emphasized [1, 2] in recent years as providing a detailed test of QCD. It is thus natural to investigate $2-\gamma$ production in the same theoretical context. As early as 1971, Berman et al. [3] discussed the QED annihilation subprocess $q\bar{q}\to\gamma\gamma$ which has the remarkable feature of being proportional to the 4th power of the quark charge. This observation stimulated further interest in studying and measuring $2-\gamma$ production in hadronic collisions.

This lowest order picture was investigated with the aim of getting informations on various fundamental features:

—(i) Quark charges: the integer charge models [4] predict considerably higher values than the standard $q\bar{q}\to\gamma\gamma$ subprocess with fractional charges.

—(ii) The value of α_s: comparing $2-\gamma$ production, via $q\bar{q}\to\gamma\gamma$, to single γ inclusive production was proposed as a means of extracting α_s. Sticking to lowest order, this comparison is meaningful only if one gets rid of the less well-known QCD Compton $qg\to q\gamma$ contribution in single γ production which involves the gluon structure function. This may be done by measuring differences of cross-sections such as $\sigma(\pi^- p\to\gamma x)-\sigma(\pi^+ p\to\gamma x)$ which isolates the QCD fusion diagram $q\bar{q}\to\gamma g$.

—(iii) The primordial parton momentum might be estimated by investigating the p_T balance of the 2 opposite photons.

—(iv) The higher order box diagram $gg\to\gamma\gamma$ was singled out as being a possibly important source of double photons in specific kinematic configurations [5].

An important piece of work remaining to be done is obviously to perform a detailed analysis, in the QCD framework, of the various contributions which should be considered in addition to $q\bar{q}\to\gamma\gamma$ (and $gg\to\gamma\gamma$). Recently, the bremsstrahlung contributions where photons are radiated from final state partons such as $qg\to\gamma(q\to\gamma)$, $q\bar{q}\to\gamma(g\to\gamma)$, have been calculated [2] in terms of the so-called "anomalous" quark and gluon fragmentation functions into photon [6]: $D_{\gamma/q}(z, Q^2)$ and $D_{\gamma/g}(z, Q^2)$. Due to the well-known behaviour of the D's: $\sim\alpha/\alpha_s(Q^2)$, these anomalous terms contribute to the same order as $q\bar{q}\to\gamma\gamma$ in the leading logarithm (LL) approximation. The largest contribution obviously comes from photons radiated off quarks; at SPS and ISR energies, it may be substantial in $\pi^+ p$ and pp collisions.

This is not, however, the full story: what about beyond leading logarithm (BLL) contributions? The

1 Laboratoire associé au Centre National de la Recherche Scientifique

aim of this paper is to analyze them, calculating the contributions of next-to-leading order diagrams: real emission diagrams $q\bar{q}\to\gamma\gamma g$, $qg\to q\gamma\gamma$ and virtual corrections to $q\bar{q}\to\gamma\gamma$.

Calculations are performed along the same line as for the corrections to the double inclusive cross-section $\sigma(\gamma p\to\gamma hx)$ [7]. We shall consider the cross-section $d\sigma/d\mathbf{p}_{T_1}dy_1dz$ where p_{T_1}, y_1 label the transverse momentum and rapidity of the trigger γ in the hadron–hadron CMS; z is defined as: $z=-\mathbf{p}_{T_2}\cdot\mathbf{p}_{T_1}/p_{T_1}^2$, $\mathbf{p}_{T_2}$ being the transverse momentum of the opposite-side photon. (This definition of z reduces in the case of the Born term $q\bar{q}\to\gamma\gamma$ and of bremsstrahlung contributions to the usual $z=p_{T_2}/p_{T_1}$). We shall also calculate $d\sigma/d\mathbf{p}_{T_1}dy_1 \quad (\bar{z}_{\min})=\int_{\bar{z}_{\min}}(d\sigma/d\mathbf{p}_{T_1}dy_1dz)\quad dz$, summing on photons with $z>\bar{z}_{\min}$.

We find that next-to-leading order diagrams contribute important corrections to the above defined cross-sections, with respect to $q\bar{q}\to\gamma\gamma$, so that double photon production cannot be described on the basis of the LL approximation only.

The choice of the variable z, to characterize the second photon, and of the corresponding observables is adapted to the experimental situation where one may look for photons which recoil against the photon trigger with a given fraction of its transverse momentum. It also has the advantage that the various effects to be studied have a different pattern when varying z: the basic $q\bar{q}\to\gamma\gamma$ sub-process has a contribution peaked at $z=1$; the $O(\alpha_s)$ corrections modify this picture, contributing substantially away from $z=1$ (the LL contribution corresponding to $qg\to\gamma(q\to\gamma)$ also contributes at $z\neq1$ but with smaller magnitude and different shape).

In a recent preprint [8], Gilmour chooses to calculate the contribution of $q\bar{q}\to\gamma\gamma g$ + virtual diagrams to the cross-section $d\sigma/d\Omega_1 d\tau$ measuring the number of γ's which recoil against a photon produced at angle θ_1 with respect to the initial beam, the 2γ invariant mass being fixed to $M^2=\tau S$. In this case, the specific pattern of $O(\alpha_s)$ corrections disappears completely and the only prediction is the ratio of the correction to the lowest order term. There is no simple way to relate this prediction to ours.

The discussion of points (i)–(iii) is better founded but more complex when considering BLL corrections. In particular extracting α_s goes through comparing the experimental ratio $[\sigma(\pi^- p\to\gamma\gamma x)-\sigma(\pi^+ p\to\gamma\gamma x)]/[\sigma(\pi^- p\to\gamma x)-\sigma(\pi^+ p\to\gamma x)]$ to the theoretical estimate which takes the form $r=(\alpha/\alpha_s(Q^2))(r_0+\alpha_s(Q^2)r_1+O(\alpha_s^2))$. Another consequence of the presence of these large corrections is that the discussion of the intrinsic parton primordial $\langle\kappa_T\rangle$ gets more delicate: one has to disentangle the effect of $\langle\kappa_T\rangle$ from the contribution of $O(\alpha_s)$ corrections in configurations when the 2 photons have unequal p_T's; so that extracting the value of $\langle\kappa_T\rangle$ from a measure of the lack of balance of the 2 photon transverse momenta is no longer a simple task.

For completeness, we shall also calculate the aplanarity distribution: $d\sigma/d\mathbf{p}_{T_1}dy_1d|p_{\text{out}}|$, characteristic of 3 jet events, where p_{out} is the momentum of the photon γ_2 perpendicular to the plane where the initial hadron and trigger photon momenta lie.

Let us finally mention that the interest of studying 2γ production is updated by the fact it may provide an important background for rare events at very high energy colliders [9].

The outline of the paper is the following: the BLL calculation is presented in Sect. II which starts by recalling the main features of the LL calculation. Section III is devoted to numerical results and discussion of the phenomenology at SPS, ISR and Sp$\bar{p}$S energies. Section IV deals with the calculation of the p_{out} distribution: $d\sigma/d\mathbf{p}_{T_1}dy_1d|p_{\text{out}}|$. Section V is devoted to the conclusion.

II. Formalism: Leading Log and Beyond Leading Log Contributions

The first part of this section will be devoted to recalling the main features of the calculation of the QED annihilation subprocess and of the other leading logarithm (LL) contributions associated to photon bremsstrahlung off partons. The second part will dwell on the BLL calculation.

1. QED Annihilation + LL Photon Bremsstrahlung

These calculations have already been reported by Berger et al. [2]. Here we shall only consider single photon bremsstrahlung (double bremsstrahlung contributions are calculated in [2] and found as expected to be very small) and give the main formulae for completeness.

We calculate the double inclusive cross-section for observing a large p_T photon γ_1 with transverse momentum and rapidity p_{T_1}, y_1 (in the CMS in the direction of the beam) together with a photon γ_2 in the opposite hemisphere, with fraction z of the trigger transverse momentum: $z=p_{T_2}/p_{T_1}$; z may be larger than 1 if the trigger photon is radiated off final partons.

In the case where the trigger photon is directly produced, the double inclusive cross-section is written, within the framework of the QCD improved parton model (neglecting primordial parton $\langle\kappa_T\rangle$) as:

$$\frac{d\sigma}{d\mathbf{p}_{T_1}dy_1dz}(h_1h_2\to\gamma_1\gamma_2X)$$
$$=\frac{1}{\pi}\sum_{abd}\int dx_1dx_2\,G_{a/h_1}(x_1,Q^2)G_{b/h_2}(x_2,Q^2)$$
$$\cdot\hat{s}\frac{d\sigma}{d\hat{t}}(a+b\to\gamma_1+d)D_{\gamma_2/d}(z,Q^2)\delta(\hat{s}+\hat{t}+\hat{u}). \quad (1)$$

The Mandelstam variables of the hadronic reaction are defined as $S=(p_{h_1}+p_{h_2})^2$, $T=(p_{h_1}-p_{\gamma_1})^2$, $U=(p_{h_2}-p_{\gamma_1})^2$; for the subprocess, $\hat{s}=(p_a+p_b)^2$, $\hat{t}=(p_a-p_{\gamma_1})^2$, $\hat{u}=(p_b-p_{\gamma_1})^2$ so that $\hat{s}=x_1x_2S$, $\hat{t}=x_1T$, $\hat{u}=x_2U$. The

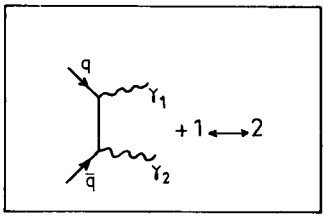

Fig. 1. QED annihilation diagram $q\bar{q}\to\gamma\gamma$

choice of Q^2 is arbitrary at the LL level. We shall show below how this arbitrariness is partly removed by including BLL corrections.

We shall consider the case where the hadrons h_1, h_2 are protons, antiprotons and pions. The definition of the partonic distributions will be discussed later on.

1a) QED Annihilation

The contribution of $q\bar{q}\to\gamma\gamma$ (Fig. 1) is obtained by putting $D_{\gamma_2/d}(z,Q^2)=\delta(1-z)$ in (1). Integrating on x_1, we find:

$$\frac{d\sigma^{\mathrm{QED}}}{d\mathbf{p}_{T_1}dy_1dz}=\frac{1}{\pi}\delta(1-z)\sum_q\int_{-T/(S+U)}^{1}\cdot\frac{dx_2}{x_2S+T}\{G_{q/h_1}(x_1,Q^2)G_{\bar{q}/h_2}(x_2,Q^2)+G_{\bar{q}/h_1}(x_1,Q^2)G_{q/h_2}(x_2,Q^2)\}\hat{s}\frac{d\sigma}{d\hat{t}}(q\bar{q}\to\gamma\gamma),\tag{2}$$

with

$$x_1=-\frac{x_2U}{x_2S+T}$$

and

$$\frac{d\sigma}{d\hat{t}}(q\bar{q}\to\gamma\gamma)=\frac{2\pi\alpha^2e_q^4}{\hat{s}^2}\frac{1}{N_C}\left(\frac{\hat{u}}{\hat{t}}+\frac{\hat{t}}{\hat{u}}\right).$$

1b) Photon Bremsstrahlung

The single γ bremsstrahlung processes are: $gq\to\gamma(q\to\gamma)$ and $q\bar{q}\to\gamma(g\to\gamma)$ (Fig. 2). They yield corrections which are of the same leading order as $q\bar{q}\to\gamma\gamma$ since the anomalous fragmentation functions behave as $\alpha/\alpha_s(Q^2)$. For $z<1$, the corresponding contribution is calculated using (1). The functions $D_{\gamma/q}(z,Q^2)$ and $D_{\gamma/g}(z,Q^2)$ describe the fragmentation of quarks and gluons into photons. They are calculable in QCD [6] and parametrizations of the LL expressions are available [10].

In the case $z>1$, corresponding to the trigger photon γ_1 being a bremsstrahlung photon, the double inclusive cross-section is given by

$$\frac{d\sigma}{d\mathbf{p}_{T_1}dy_1dz}(h_1h_2\to\gamma_1\gamma_2X)=\frac{1}{\pi}\sum_{abd}\int dx_1dx_2G_{a/h_1}(x_1,Q^2)G_{b/h_2}(x_2,Q^2)$$

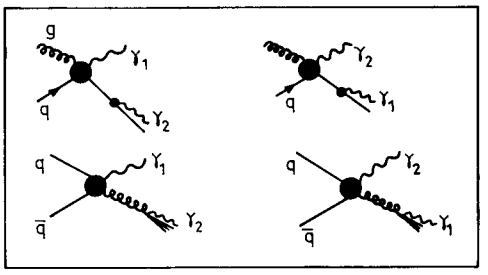

Fig. 2. The single γ bremsstrahlung processes

$$\cdot\hat{s}\frac{d\sigma}{d\hat{t}}(a+b\to\gamma_2+d)D_{\gamma_1/d}\left(\frac{1}{z},Q^2\right)\cdot\theta(z-1)\delta(\hat{s}+\hat{t}+\hat{u})\tag{3}$$

with $\hat{s}=x_1x_2S$, $\hat{t}=(p_a-p_{\gamma_2})^2=(p_b-p_d)^2=x_2Uz$, $\hat{u}=x_1Tz$. The QCD subprocess cross-sections $d\sigma/d\hat{t}(qg\to q\gamma)$ and $d\sigma/d\hat{t}$ $(q\bar{q}\to\gamma g)$ are given in Appendix A.

Due to the trigger bias effect, the contribution for $z>1$ is much smaller than for $z<1$. On the other hand, the gluon fragmentation into photon contributes little.

As was pointed out by several authors [5], the higher order diagrams $gg\to\gamma\gamma$ may lead to an important contribution in specific kinematic situations. Similarly to $q\bar{q}\to\gamma\gamma$, it corresponds to equal p_T configurations for the 2 photons. We refer the reader to [2] for useful formulae and postpone the discussion of this contribution to Sect. III.

2. Beyond Leading Logarithm Contributions

The technique of such calculations is inspired from the method we have already developed in calculating BLL corrections to the double inclusive cross-section $d\sigma^{(\gamma p\to\gamma hx)}/d\mathbf{p}_Tdydx_h$ for observing a large p_T photon together with a hadron h in the opposite hemisphere with fraction x_h of the trigger transverse momentum [7].

In the present case, we shall perform the calculation of BLL corrections corresponding to the higher order diagrams drawn in Fig. 3: $q\bar{q}\to\gamma\gamma g$ + interference terms between lowest order and virtual $O(\alpha_s)$ correction to $q\bar{q}\to\gamma\gamma$, and $qg\to q\gamma\gamma$.

Let us start, as usual, from the parton model expression for the double inclusive cross-section:

$$\frac{d\sigma^0}{d\mathbf{p}_{T_1}dy_1dz}=\delta(1-z)\frac{1}{\pi}\sum_{i=q,\bar{q}}\cdot\int dx_1dx_2G^0_{i/h_1}(x_1)G^0_{\bar{i}/h_2}(x_2)\cdot\hat{s}\frac{d\sigma}{d\hat{t}}(i+\bar{i}\to\gamma_1+\gamma_2)\delta(\hat{s}+\hat{t}+\hat{u}),\tag{4}$$

where z is defined in the CMS system as $z=$

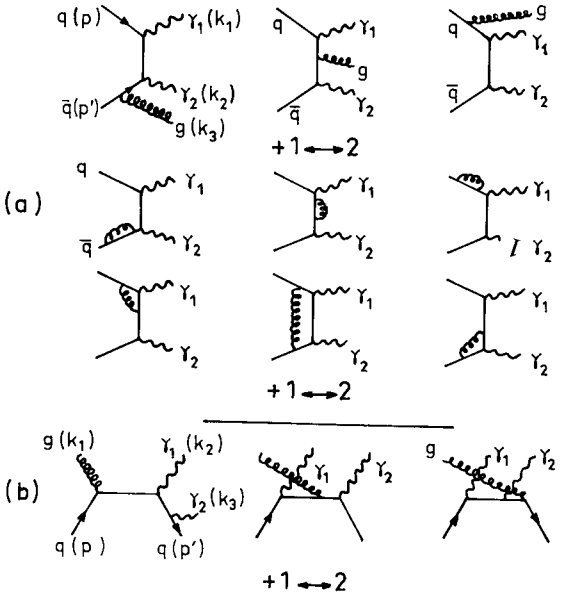

Fig. 3. **a** real and virtual $O(\alpha_s)$ diagrams with $q\bar{q}$ initial partons, **b** real $O(\alpha_s)$ diagrams with gq initial partons

$-\mathbf{p}_{T_2}\cdot\mathbf{p}_{T_1}/p_{T_1}^2$ and the G^0's are bare parton distribution functions. Including parton cross-sections to order α_s, corresponding to diagrams of Fig. 3, leads to

$$\frac{d\sigma}{d\mathbf{p}_{T_1}dy_1dz}=\frac{d\sigma^0}{d\mathbf{p}_{T_1}dy_1dz}+\frac{d\sigma^1}{d\mathbf{p}_{T_1}dy_1dz}, \tag{5}$$

with

$$\begin{aligned}\frac{d\sigma^1}{d\mathbf{p}_{T_1}dy_1dz}=&\frac{1}{\pi}\sum_{i=q,\bar{q}}\int dx_1\frac{dx_2}{\hat{s}}G^0_{i/h_1}(x_1)G^0_{\bar{i}/h_2}(x_2)\\&\cdot\frac{\alpha_s}{2\pi}\theta(\hat{s}+\hat{t}+\hat{u})k_{i\bar{i}}(\hat{s},\hat{t},\hat{u},z)\\&+\frac{1}{\pi}\sum_{i,j=q,g}\int dx_1\frac{dx_2}{\hat{s}}G^0_{i/h_1}(x_1)G^0_{j/h_2}(x_2)\\&\cdot\frac{\alpha_s}{2\pi}\theta(\hat{s}+\hat{t}+\hat{u})k'_{ij}(\hat{s},\hat{t},\hat{u},z),\end{aligned} \tag{6}$$

where k and k' refer to contributions of Figs 3a and b respectively, with $q\bar{q}$ and qg initial partons. α_s is a short hand notation for $\alpha_s(\mu^2)$, μ being an arbitrary scale introduced through dimensional regularization, and will be used from now on. The expressions for k and k' contain singular terms which can be factored out and absorbed in the bare distributions, building the scaling violating partonic distributions which depend on a large factorization scale Q^2 [11]. From now on, we take $\mu^2=Q^2$; the specific definition of Q^2 will be discussed in Sect. III. This procedure leads to:

$$\frac{d\sigma}{d\mathbf{p}_{T_1}dy_1dz}=d\sigma^{(\mathrm{LL})}+d\sigma^{(\mathrm{BLL})}, \tag{7}$$

where $d\sigma^{(\mathrm{LL})}$ is the full leading logarithm contribution (QED + bremsstrahlung) calculated in 1.) and the beyond leading logarithm correction $d\sigma^{(\mathrm{BLL})}$ is given by:

$$d\sigma^{(\mathrm{BLL})}=d\sigma^{(\mathrm{BLL})}_{q\bar{q}}+d\sigma^{(\mathrm{BLL})}_{qg}, \tag{8}$$

and

$$\begin{aligned}\frac{d\sigma^{(\mathrm{BLL})}_{q\bar{q}}}{d\mathbf{p}_{T_1}dy_1dz}=&\frac{1}{\pi}\sum_{i=q,\bar{q}}\int dx_1\\&\cdot\frac{dx_2}{\hat{s}}G_{i/h_1}(x_1,Q^2)G_{\bar{i}/h_2}(x_2,Q^2)\\&\cdot\frac{\alpha_s(Q^2)}{2\pi}\theta(\hat{s}+\hat{t}+\hat{u})K_{i\bar{i}}(\hat{s},\hat{t},\hat{u},Q^2,z),\end{aligned} \tag{9}$$

where K is now free from singularities. An analogous formula holds for $d\sigma^{(\mathrm{BLL})}_{qg}$.

Let us introduce the variables V, W [12] to describe the hadronic cross-section: $W=-U/(S+T)$, $V=1+T/S$. The parton process is described correspondingly by variables $\hat{s}$, v, w. Expressing x_1 and x_2 in terms of v, w:

$$x_1=\frac{VW}{vw},\quad x_2=\frac{1-V}{1-v}, \tag{10}$$

equation (9) is easily rewritten as:

$$\begin{aligned}\frac{d\sigma^{(\mathrm{BLL})}_{q\bar{q}}}{d\mathbf{p}_{T_1}dy_1dz}=&\frac{1}{\pi}\frac{1}{p^4_{T_1}}\sum_{i=q,\bar{q}}\int_{VW}^{V}dv\\&\cdot\int_{VW/v}^{1}dw x_1G_{i/h_1}(x_1,Q^2)\\&\cdot x_2G_{\bar{i}/h_2}(x_2,Q^2)\hat{s}v^2w(1-v)\\&\cdot\frac{\alpha_s(Q^2)}{2\pi}K_{i\bar{i}}(\hat{s},v,w,z,Q^2).\end{aligned} \tag{11}$$

In the case of $d\sigma^{(\mathrm{BLL})}_{qg}$, kinematics is somehow complicated by the lack of symmetry between quark and gluon. At the parton level, we shall define the kinematics as $\hat{t}=(p_g-p_{\gamma_1})^2$, $\hat{u}=(p_q-p_{\gamma_1})^2$ so that in the case where we consider the gluon in hadron h_2, relations (10) between x_1, x_2 and v, w should be replaced by:

$$x_1=\frac{VW}{1-v},\quad x_2=\frac{1-V}{vw}, \tag{12}$$

we then write $d\sigma^{(\mathrm{BLL})}_{qg}$ as the sum of 2 terms:

$$\frac{d\sigma^{(\mathrm{BLL})}_{qg}}{d\mathbf{p}_{T_1}dy_1dz}=d\sigma^{(1)}+d\sigma^{(2)}, \tag{13}$$

with

$$\begin{aligned}d\sigma^{(1)}=&\frac{1}{\pi}\frac{1}{p^4_{T_1}}\sum_{i=q,\bar{q}}\int_{VW}^{V}dv\int_{VW/v}^{1}dw x_1G_{g/h_1}(x_1,Q^2)\\&\cdot x_2G_{i/h_2}(x_2,Q^2)\hat{s}v^2w(1-v)\frac{\alpha_s(Q^2)}{2\pi}\\&K'_{gi}(\hat{s},v,w,z,Q^2),\end{aligned} \tag{14}$$

where x_1, x_2 are given by (10)

and

$$d\sigma^{(2)}=\frac{1}{\pi}\frac{1}{p_{T_1}^4}\sum_{i=q,\bar{q}}\int_{1-V}^{1-VW}dv\int_{(1-V)/v}^{1}dw\,x_1G_{i/h_1}(x_1,Q^2)\cdot x_2G_{g/h_2}(x_2,Q^2)\hat{s}v^2w(1-v)\frac{\alpha_s(Q^2)}{2\pi}\cdot K'_{gi}(\hat{s},v,w,z,Q^2), \tag{15}$$

where x_1 and x_2 are given by (12)

In order to extract the genuine higher order corrections $K_{i\bar{i}}$ and K'_{g_i} from the perturbative expressions of $k_{i\bar{i}}$ and k'_{g_i}, one has to use the implications of factorization and as explained at length in [12, 7], introduce a choice of definitions for the distribution functions.

2a) *Definition of the Partonic Distributions*

In the case of $q\bar{q}\to\gamma\gamma g$, the singular terms which we encounter and which should be subtracted and absorbed in the bare distributions are associated with the quark and antiquark distributions.

On the other hand, in the case of $qg\to q\gamma\gamma$, the singular terms are linked to the quark fragmenting into photon and to the quark distribution.

Let us briefly recall the difference between the 2 usual conventions for the definition of the parton distributions inside the nucleon. In deep inelastic scattering, the quark distribution in the nucleon, calculated perturbatively to order α_s is written as:

$$G_{q/p}(x,Q^2)=G^0_{q/p}(x)+\frac{\alpha_s}{2\pi}\int_0^1dy\int_0^1dz\,\delta(zy-x)\cdot\{G^0_{q/p}(y)H_{qq}(z,Q^2)+G^0_{g/p}(y)H_{qg}(z,Q^2)\}, \tag{16}$$

where H_{qq} (H_{qg}) are given [13] by the sum of a singular term and of a finite $O(\alpha_s)$ contribution*:

$$\frac{\alpha_s}{2\pi}H_{\substack{qq\\qg}}(z,Q^2)=-\frac{1}{\varepsilon}\frac{\alpha_s}{2\pi}P_{\substack{qq\\qg}}(z)\cdot\left(\frac{4\pi\mu^2}{Q^2}\right)^{\varepsilon}\frac{\Gamma(1-\varepsilon)}{\Gamma(1-2\varepsilon)}+\alpha_s\bar{f}_{\substack{qq\\qg}}+O(\varepsilon). \tag{17}$$

The non singular $O(\alpha_s)$ term depends on the choice of the factorization convention. The non universal convention [13, 14] requiring that all higher order corrections to the deep inelastic scattering structure function F_2 are absorbed in the definition of the parton distributions, leads to $\bar{f}_{\substack{qq\\qg}}\neq 0$ [13]. On the other hand, the universal convention [16] corresponds to $\bar{f}_{\substack{qq\\qg}}=0$.

The choice of the non universal convention is convenient for quark distributions extracted from deep inelastic data in the LL approximation. Concerning the anomalous fragmentation functions of quarks and gluons into photons, we use in (1) and (3) the available parametrization [10] to theoretical leading logarithm QCD expressions [6]. Therefore, to order α_s, we consistently remove the collinear singularities, in the perturbative calculations by factorizing the distribution:

$$\frac{\alpha}{2\pi}\tilde{H}_{\gamma q}(z,Q^2)=-\frac{1}{\varepsilon}\frac{\alpha}{2\pi}P_{\gamma q}(z)\left(\frac{4\pi\mu^2}{Q^2}\right)^{\varepsilon}\frac{\Gamma(1-\varepsilon)}{\Gamma(1-2\varepsilon)}. \tag{18}$$

2b) *Extracting the BLL Correction from Perturbative Expressions*

Comparing (5) and (7) and using (16)–(18), we write down the relations implied by factorization between $K(K')$ and the perturbative expressions $k(k')$:

$$\frac{\alpha_s}{2\pi}K_{q\bar{q}}(\hat{s},v,w,z,Q^2)=\frac{\alpha_s}{2\pi}k_{q\bar{q}}(\hat{s},v,w,z)-\frac{\alpha_s}{2\pi}\left\{\frac{1}{1-vw}H_{qq}\left(\frac{1-v}{1-vw},Q^2\right)\cdot\frac{d\sigma^{q\bar{q}\to\gamma\gamma}}{dv}\left(\frac{1-v}{1-vw}\hat{s},vw\right)\delta(1-z)\right\}-\frac{\alpha_s}{2\pi}\left\{\frac{1}{v}H_{qq}(w,Q^2)\frac{d\sigma^{q\bar{q}\to\gamma\gamma}}{dv}(w\hat{s},v)\delta(1-z)\right\}. \tag{19}$$

Similarly, we find:

$$\frac{\alpha_s}{2\pi}K'_{gq}=\frac{\alpha_s}{2\pi}k'_{gq}-\frac{\alpha}{2\pi}\left\{\frac{1}{1-v+vw}\tilde{H}_{\gamma q}(1-v-vw,Q^2)\cdot\frac{d\sigma^{g+q\to\gamma+q}}{dv}\left(\hat{s},\frac{1-v}{1-v+vw}\right)\cdot\delta(z_1-z)\right\}-\frac{\alpha_s}{2\pi}\left\{\frac{1}{v}\tilde{H}_{\gamma q}(z,Q^2)\frac{d\sigma^{g+q\to\gamma+q}}{dv}(\hat{s},v)\delta(1-w)\right\}-\frac{\alpha_s}{2\pi}\left\{\frac{1}{vw}H_{qg}(w,Q^2)\frac{d\sigma^{q+\bar{q}\to\gamma+\gamma}}{dv}(w\hat{s},v)\delta(1-z)\right\}, \tag{20}$$

where $z_1=1/(1-v+vw)$.

The n dimensional expressions for the various Born terms $(d\sigma/dv)(s,v)$ appearing in (19) and (20) may be found in Appendix A. Notice in (20) the singular term $\delta(z_1-z)$ corresponding to collinear kinematics for the trigger photon γ_1 radiated off the final quark.

Let us finally remark that the total spectrum given by (7) using (19) and (20) does not depend on Q^2 to order α_s: this is a result of factorization [11]. For instance, the Q^2 dependence of the scaling violating distributions, expressed to order α_s through (16) is cancelled by a corresponding term in $K_{q\bar{q}}$ (19). The distributions which enter (7) have, however, an implicit Q^2 dependence to all orders in α_s—which leaves us with a Q^2 dependence of the final result. Although cancelling a large part of the arbitrariness in the choice of Q^2, compared to the LL approximation, the inclu-

* The mass singularities are regularized by working in the dimensional regularization [15] scheme with the number of space–time dimensions $n=4-2\varepsilon$

sion of BLL corrections does not completely remove it. This will be discussed later on in Sect. III.

2c) Calculation of k and k'

The variable z describes the double inclusive cross-section both at the hadronic and at the partonic level. We may write the perturbative expression k as the sum of $O(\alpha_s)$ virtual elastic and real inelastic partonic cross-sections:

$$\frac{\alpha_s}{2\pi}k(\hat{s},v,w,z)=\frac{1}{v}\frac{d\sigma^{\text{virtual}}}{dv}(\hat{s},v)\delta(1-w)\delta(1-z)+\frac{1}{v}\frac{d\sigma^{q+\bar{q}\to\gamma+\gamma+g}}{dvdwdz}(\hat{s},v,w,z)\theta(1-w), \quad (21)$$

and similarly for k':

$$\frac{\alpha_s}{2\pi}k'(\hat{s},v,w,z)=\frac{1}{v}\frac{d\sigma^{g+q\to\gamma+\gamma+q}}{dvdwdz}(\hat{s},v,w,z)\theta(1-w). \quad (22)$$

The inelastic contribution is obtained by integrating the matrix element squared corresponding to real diagrams drawn in Fig. 3 on appropriate phase-space (see Appendix B). In addition to singular functions in w, it contains singular functions in z: $\delta(1-z)$, $(1/(1-z))_+ \cdot\theta(1-z),\ldots$ and $\delta(z_1-z)$, $(1/(z_1-z))_+\ \theta(z_1-z),\ldots$ in the case of $qg\to q\gamma\gamma$. The overall result is therefore rather involved. We shall treat k and k' separately, leaving technical details for Appendix B.

i) Calculation of the Inelastic Diagram $q\bar{q}\to\gamma\gamma g$ contribution. It follows closely [7]. The invariants a_i, b_i in terms of which the squared matrix element $|M_{q\bar{q}}|^2$ is calculated are defined as usual:

$$a_i=p\cdot k_i,\quad b_i=p'\cdot k_i, \quad (23)$$

with $p\cdot p'=a_1+a_2+a_3=b_1+b_2+b_3\equiv\hat{s}/2$. Notice that $a_1\equiv-\hat{t}/2$, $b_1\equiv-\hat{u}/2$, $a_2+a_3=(\hat{s}+\hat{t})/2$, $b_2+b_3=(\hat{s}+\hat{u})/2$ and $\hat{s}+\hat{t}+\hat{u}=(k_2+k_3)^2=s_2$.

It is easy to obtain $|M_{q\bar{q}}|^2=|M(q\bar{q}\to\gamma\gamma g)|^2$ from $|M(\gamma q\to\gamma qg)|^2$ by crossing applied to (36) of [7]. (The colour factor for the colour and spin averaged matrix element squared is now C_F/N_C.)

Analogously to [7], it is convenient to define

$$z=\frac{(p\cdot p')(k_1\cdot k_2)-(k_1\cdot p)(p'\cdot k_2)-(p\cdot k_2)(k_1\cdot p')}{2(k_1\cdot p)(k_1\cdot p')}=\frac{(P\cdot P')(k_1\cdot k_2)-(k_1\cdot P)(P'\cdot k_2)-(P\cdot k_2)(k_1\cdot P')}{2(k_1\cdot P)(k_1\cdot P')} \quad (24)$$

(where $P=p_{h_1}$, $P'=p_{h_2}$), which is nothing else than $z=-\mathbf{p}_{T_1}\cdot\mathbf{p}_{T_2}/p_{T_1}^2$ in a frame in which the incident hadrons are collinear and define the longitudinal axis ($z=p_{T_2}/p_{T_1}$ in the case of $2\to2$ kinematics as in part 1 of this section).

By keeping $z>0$, we avoid the singularities due to a_2 and b_2 which vanish when $z=0$. The requirement $z>0$ also constrains $\mathbf{p}_2$ to lie in the opposite hemisphere with respect to γ_1.

We may define m such that $z\equiv m\cdot k_2$: $m=(\hat{s}k_1+\hat{t}p'+\hat{u}p)/\hat{t}\hat{u}$ and $m^2=-\hat{s}/\hat{t}\hat{u}$, $m\cdot k_1=-1$, $m\cdot p=mp'=0$, which leads to $z=1-m\cdot k_3$. The variable z may thus be larger than 1 (recoiling γ_2 balanced by γ_1 + gluon). The maximum value of z is calculated in Appendix B:

$$z_{\max}=\frac{1}{2}\left(1+\sqrt{\frac{1-vw}{w(1-v)}}\right) \quad (25)$$

The n dimensional phase-space integrations which lead to $d\sigma/dvdwdz$ are worked out in Appendix B.

ii) Virtual Gluon Corrections to the Basic $q\bar{q}\to\gamma\gamma$ Subprocess. The $O(\alpha_s)$ virtual correction is obtained as the interference term of the Born diagrams (Fig. 1) and of the virtual diagrams of Fig. 3a. We show in Appendix A how starting from the corresponding expression for $\gamma q\to\gamma q$ given in [7], we may perform appropriate crossing in order to get* $(d\sigma^{\text{virtual}}/dv)(\hat{s},v)$:

$$\frac{d\sigma^{\text{virtual}}}{dv}(\hat{s},v)=\frac{\alpha_s}{2\pi}\frac{C_F}{N_C}\frac{\Gamma(1-\varepsilon)}{\Gamma(1-2\varepsilon)}F(\hat{s},v,\varepsilon)\cdot\left\{\left(\frac{4\pi\mu^2}{\hat{s}}\right)^{\varepsilon}\left[\left(-\frac{2}{\varepsilon^2}+\frac{1}{\varepsilon}\right)\left(\frac{1-v}{v}+\frac{v}{1-v}\right)+\frac{4}{\varepsilon}\right]+\left(\frac{1-v}{v}+\frac{v}{1-v}\right)\left(\tfrac{2}{3}\pi^2-3+\ln^2 v+\ln^2(1-v)+3\ln(1-v)\right)+2+2\ln v+2\ln(1-v)+\frac{3(1-v)}{v}(\ln v-\ln(1-v))+\left(2+\frac{v}{1-v}\right)\ln^2 v+\left(2+\frac{1-v}{v}\right)\ln^2(1-v)\right\}, \quad (26)$$

where

$$F(\hat{s},v,\varepsilon)=\frac{2\pi\alpha^2e_q^4}{\hat{s}}\mu^{2\varepsilon}\frac{1}{\Gamma(1-\varepsilon)}\left(\frac{4\pi\mu^2}{\hat{s}v(1-v)}\right)^{\varepsilon}.$$

Adding virtual and real contributions in (20), one readily verifies that the singular terms proportional to $1/\varepsilon^2$ cancel.

iii) The Calculation of the Inelastic Diagrams $qg\to q\gamma\gamma$ Contribution is done with the same matrix element as $\gamma q\to\gamma qg$ [7] (up to the colour factor $1/(N_C^2-1)$ for the completely colour and spin averaged matrix element squared). With $a_i=p\cdot k_i$, $b_i=p'\cdot k_i$ (see Fig. 3b), we notice that $p\cdot p'=a_1-a_2-a_3=-b_1+b_2+b_3$, $a_1=\hat{s}/2$, $a_2=-\hat{u}/2$, $b_3=(\hat{s}+\hat{t}+\hat{u})/2=s_2/2$.

The definition of the variable z is changed however with respect to the Compton case since we now observe both photons. This leads to $z=m\cdot k_3=1-m\cdot p'$ with $m=(\hat{s}k_2+\hat{t}p+\hat{u}k_1)/\hat{t}\hat{u}$ and $m\cdot k_1=m\cdot p=0$, $m\cdot k_2=-1$.

Integrating on phase space, collinear singularities associated with $b_1=0$, $b_2=0$ are encountered corresponding respectively to singularities at $z=1$ and $z=z_1=1/(1-v+vw)$. This last one which corresponds

* As for $\gamma q\to\gamma q$, there are no uv divergences. No counter terms are needed

to collinear kinematics for the trigger γ_1 radiated from the final quark, is new with respect to the Compton case. So that the singularity structure of k' is somehow more complicated than for k (see Appendix B). (In this case there are no $1/\varepsilon^2$ terms at the level of inelastic contribution, in the absence of associated virtual terms.)

We may now use (19) and (20) in order to calculate $K_{q\bar{q}}$ and K_{qg}, verifying that all singular $1/\varepsilon$ terms cancel, leading, as expected, to finite BLL corrections.

2d) Calculation of Double Inclusive Cross-Sections

Using expressions (8)–(15) we obtain the (BLL) corrections to $d\sigma/d\mathbf{p}_{T_1}dy_1dz$. Due to the singular structure of K and K', these are, however, distributions in z, containing, as displayed in Appendix B, terms such as $\delta(1-z)$,

$$\left(\frac{1}{1-z}\right)_+\theta(1-z),\left(\frac{1}{z-1}\right)_+\theta(z-1),\delta(z_1-z),$$
$$\cdot\left(\frac{1}{z_1-z}\right)_+\theta(z_1-z),\left(\frac{1}{z-z_1}\right)_+\theta(z-z_1),\ldots$$

These distributions are, of course, smoothed out as soon as the experimental resolution is taken into account. We shall thus define physical double inclusive cross-sections as:

$$\frac{d\sigma}{d\mathbf{p}_{T_1}dy_1}(\bar{z}_{\min})=\int_{\bar{z}_{\min}}^{z_{\max}}dz\frac{d\sigma}{d\mathbf{p}_{T_1}dy_1dz}, \tag{27}$$

and

$$\frac{d\sigma}{d\mathbf{p}_{T_1}dy_1dz}(\Delta z)$$
$$\equiv\frac{1}{\Delta z}\int_{z-\Delta z/2}^{z+\Delta z/2}dz'\frac{d\sigma}{d\mathbf{p}_{T_1}dy_1dz'}$$
$$=\frac{1}{\Delta z}\left[\frac{d\sigma}{d\mathbf{p}_{T_1}dy_1}\left(z+\frac{\Delta z}{2}\right)\right.$$
$$\left.-\frac{d\sigma}{d\mathbf{p}_{T_1}dy_1}\left(z-\frac{\Delta z}{2}\right)\right] \tag{28}$$

where Δz defines some chosen binning, $\bar{z}_{\min}$ is an arbitrary experimental cut and $z_{\max}$ is the maximum value of z in the available phase-space.

For $\bar{z}_{\min}<1$, in order to use (27)–(28), we have however to take care of the fact that the distributions $1/(1-z)_+$, $1/(z_1-z)_+$ are defined in the integration range $0<z<1$ and $0<z<z_1$ respectively. It is convenient to introduce more general distributions: $(1/(1-z))_{\bar{z}_{\min}}$ such that

$$\int_{\bar{z}_{\min}}^{1}\frac{f(z)dz}{(1-z)_{\bar{z}_{\min}}}=\int_{\bar{z}_{\min}}^{1}\frac{f(z)-f(1)}{1-z}dz$$

with $1/(1-z)_+=1/(1-z)_{\bar{z}_{\min}}+\ln(1-\bar{z}_{\min})\delta(1-z)$ and similarly for $1/(z_1-z)_+$. For $z_{\min}>1$, the distribution $1/(z-1)_+\ \theta(z-1)$ is simply replaced by $1/(z-1)$ which produces terms proportional to $\ln(\bar{z}_{\min}-1)$.

These substitutions make explicit the presence of logarithmic singularities when $\bar{z}_{\min}\to 1\cdot\pm 0$, which indicates a breakdown of the perturbative approach; for $z_{\min}$ close to 1, these large logarithms should be resumed to all orders.

III. Numerical Results

We begin this section by describing the structure functions we use in our numerical calculations, as well as the factorization conventions we adopt when computing the BLL corrections. The scale in the structure functions and in the coupling constant

$$\alpha_s(Q^2)=\frac{12\pi}{25\ln\dfrac{Q^2}{\Lambda^2}},\quad \Lambda=0.2\,\text{GeV}, \tag{29}$$

is

$$Q^2=p_{T_1}^2. \tag{30}$$

We postpone to the end of this section the discussion of the arbitrariness in the choice of the scale.

For the proton, the valence and sea quark distributions are taken from [17], and the gluon distribution from [18]. For the quark and gluon distributions within the pion, we use the parametrization given by Owens (set I of [19]).

Since the proton distributions* are obtained from LL fits to the data [18, 20], we have to use, for consistency, expression (17) with $\bar{f}_{qq}$ and $\bar{f}_{qg}$ given in [14]. For the pion, we adopt the same convention. The fragmentation functions $D_{\gamma/q}$ and $D_{\gamma/g}$ are borrowed from Nicolaidis [10].

1. $\pi^- p\to\gamma\gamma X$ at SPS energy

The cross-section** $d\sigma(\bar{z}_{\min}=0.5)/d\mathbf{p}_T dy$ for the reaction $\pi^- p\to\gamma\gamma X$ is shown in Fig. 4 as a function of p_T at $E^{\pi}_{\text{LAB}}=300$ GeV. The dotted curve is the Born contribution, whereas the full curve shows the totally corrected spectrum (Born + Box + LL + BLL contributions). The relative importance of the Box, LL and BLL contributions is shown in Fig. 5 where the ratios Box/Born, LL/Born and BLL/Born are plotted. The BLL/Born ratio is large and almost constant with p_T, whereas the Box and LL contributions are smaller and fastly decreasing with increasing p_T. Therefore in these energy and p_T ranges, the BLL contribution is *the most important correction* to the Born term.

It is interesting to look at the cross-section variation with z or $\bar{z}_{\min}$ at fixed p_T; the integrated BLL correction $d\sigma^{\text{BLL}}(\bar{z}_{\min})/d\mathbf{p}_T dy$ is shown in Fig. 6 and the differen-

* Strictly speaking, it is the definition $F_3=\sum^{q=\text{val}} G_q(x,Q^2)$ which is used in [17, 18]; this corresponds to a minor change in the functions $\bar{f}_{ij}(x)$

** p_T and y is a shorthand notation for p_{T_1} and y_1

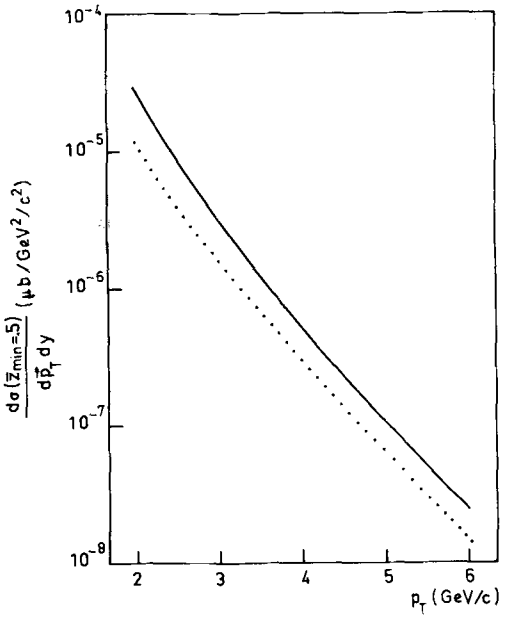

Fig. 4. $d\sigma(\bar{z}_{min}=0.5)/dy d\mathbf{p}_T$ as a function of p_T, for $\pi^- p \to \gamma\gamma X$, $E^{\pi}_{Lab}=300$ GeV, $y=0$. The dotted (full) curve corresponds to the Born term (fully corrected: Born + Box + LL + BLL contributions)

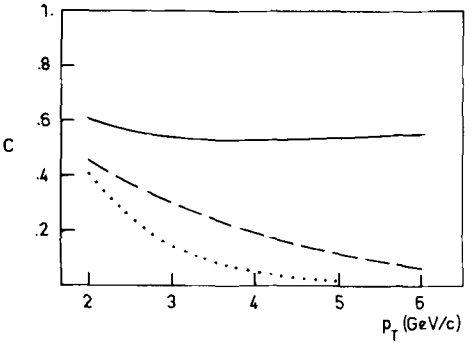

Fig. 5. Ratios Box/born (dotted), LL/Born (dashed), BLL/Born (full) as functions of p_T for $\pi^- p \to \gamma\gamma X$, $E^{\pi}_{Lab}=300$ GeV, $y=0$

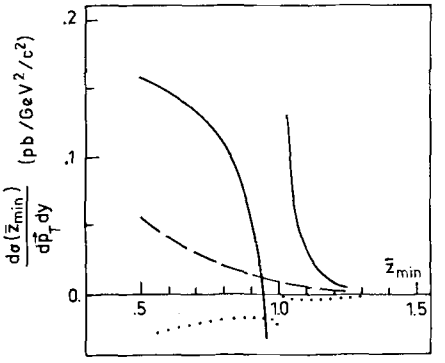

Fig. 6. $d\sigma(\bar{z}_{min})/dy d\mathbf{p}_T$ as a function of $\bar{z}_{min}$, at $p_T=4$ GeV/c for $\pi^- p \to \gamma\gamma X$, $E^{\pi}_{Lab}=300$ GeV, $y=0$. The full curve is the total BLL contribution, the dotted curve corresponds to $gq \to \gamma\gamma q$, the dashed curve to the LL contributions

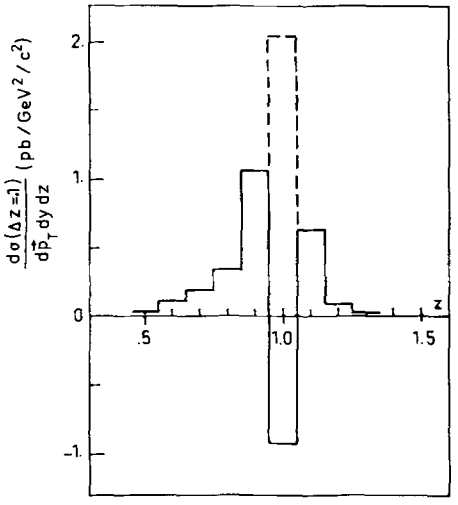

Fig. 7. $d\sigma(\Delta z)/d\mathbf{p}_T dy dz$ as a function of z at $p_T=4$ GeV/c for $\pi^- p \to \gamma\gamma X$, $E^{\pi}_{Lab}=300$ GeV, $y=0$ with bins $\Delta z=0.1$. The full curve is the BLL contribution; the dashed curve is the contribution Born + BLL in the bin around $z=1$

tial spectrum $d\sigma^{BLL}(\Delta z)/d\mathbf{p}_T dy dz$ (28) in Fig. 7 for $p_T=4$ GeV/c. For this value of p_T and for $\bar{z}_{min}<1$, we obtain $d\sigma^{BORN}(\bar{z}_{min})/d\mathbf{p}_T dy=0.296$ pb/GeV^2/c^2. We notice that the integrated cross-sections strongly varies with $\bar{z}_{min}$; on Fig. 6 the correction blows up when $\bar{z}_{min}$ goes to 1. This is due to the presence of the logarithmic singularities in the BLL corrections as discussed in Sect. II. Therefore our calculation to order $O(\alpha_s)$ becomes no more reliable for $\bar{z}_{min}$ too close to 1 (when $|d\sigma^{BLL}(\bar{z}_{min})/d\mathbf{p}_T\,dy| \simeq d\sigma^{BORN}/d\mathbf{p}_T dy$). We shall discuss this limitation when considering the differential spectrum.

Also shown on Fig. 6 are the LL contribution (dashed curve) and the contribution (dotted curve) to the BLL corrections coming from the "Compton graphs" ($gq \to \gamma\gamma q$) alone; this latter is small.

Let us finally notice that the BLL corrections are not sensitive to the inclusion or not of the functions $\bar{f}_{ij}(z)$ in (17) (since they vary by less than 10%).

The differential BLL correction is shown for a binning $\Delta z=0.1$ in Fig. 7; the correction is negative at $z=1$. When the Born term is added, we get the dashed curve which is, together with the full line at $z \neq 1$, the fully corrected cross-section. (We have neglected the Box and LL contributions, the latter being non negligible only at small z). Without BLL corrections, we would get a large peak at $z=1$ due to the Born term. The BLL correction widens the peak while decreasing its height.

The corresponding curves for $p_T=2$ GeV/c are shown in Figs 8 and 9. In Fig. 8 the contribution of the Box diagram (dotted line) is also included. These various contributions are now of the order of the Born term (dashed-dotted line)

As remarked already in Sect. II, when $\bar{z}_{min}$ is close to $\bar{z}_{min} \simeq 1$ an infrared sensitive region is approached. The

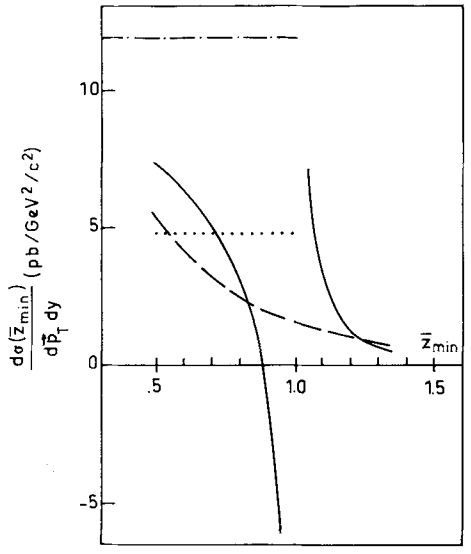

Fig. 8. Same as on Fig. 6 but for $p_T = 2$ GeV/c; the dotted (dash-dotted) curve is the Box (Born) diagram contribution

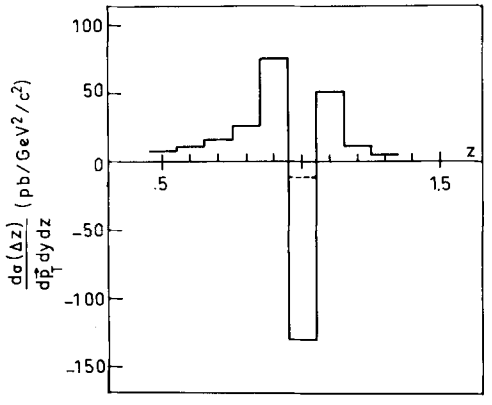

Fig. 9. Same as on Fig. 7, but for $p_T = 2$ GeV/c

BLL correction (Fig. 9) becomes negative and even larger in magnitude than the Born term. In the extreme limit of almost perfect resolution $\Delta z \to 0$ at $z = 1$, the leading behaviour of the differential cross-section (28) may be derived as

$$\frac{d\sigma(\Delta z)}{d\mathbf{p}_T dy dz} \xrightarrow[\Delta z \to 0]{z=1} \frac{1}{\Delta z}\frac{d\sigma^{\mathrm{BORN}}}{d\mathbf{p}_T dy}\left[1 - \frac{2\alpha_s}{\pi} C_F \ln^2\left(\frac{\Delta z}{2}\right)\right] + O\left(\alpha_s \ln\frac{\Delta z}{2}\right). \tag{31}$$

As it is familiar from other processes a double logarithm due to soft gluon emission [21] appears, indicating that finite order perturbation theory breaks down for this specific configuration. Therefore resummation techniques have to be applied. When summing just the double logs (with fixed α_s) an exponential damping by $\exp[-2\alpha_s/\pi\ C_F \ln^2(\Delta z/2)]$ of the above cross-section is to be expected. But because of this suppression semi-

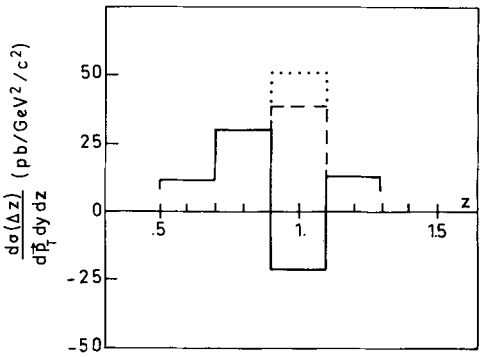

Fig. 10. Same as Fig. 9 but with a different binning $\Delta z = 0.2$. The dotted curve is the Born + Box + BLL contribution in the bin around $z = 1$

hard gluon emissions have to be taken into account and resummed, as it was first pointed out by Parisi and Petronzio [22] for the case of the transverse momentum distribution in the Drell–Yan process. Correspondingly a sensible and non-vanishing $d\sigma(\Delta z)/d\mathbf{p}_T dy dz$ at $z = 1$ would result even for very small values of Δz.

Since in this paper we concentrate on the $O(\alpha_s)$ terms only, we consequently have to demand that the binning in Δz does not become too small in order to prevent the breakdown of the finite order calculation. For the case with $p_T = 2$ GeV/c (Fig. 9) the value $\Delta z = 0.1$ is evidently too small. A larger binning is therefore required. Figure 10 shows the result for $\Delta z = 0.2$. The prediction is now reliable, but a sharp resolution in z is lost. The dotted line in Fig. 10 is obtained by adding the Box term.

Up to now, we have not taken into account the smearing due to the primordial transverse momentum κ_T of the incident partons. This latter also widens the Born term peak. It is therefore not easy to disentangle the smearing effect from the BLL corrections.

We can estimate the effect of the primordial smearing on the Born contribution with the following simple model. The unsmeared Born term behaves as $d\sigma^{\mathrm{Born}}/dz \sim \delta(1-z)$. Including parton primordial κ_T we obtain $d\sigma^{\mathrm{Born}}/dz \sim \delta(p'_T/p_T - z) = \delta((p_T - \kappa_{Tx})/p_T - z)$ where the momenta are defined in Fig. 11; we only consider the smearing in the scattering plane with κ_{T_x} being the sum of the parton transverse momenta. We describe the effective κ_T distribution by

$$\frac{dN}{d\kappa_T} = \frac{A}{\pi} e^{-A(\kappa_{Tx} - \bar{\kappa})^2} e^{-A\kappa_{Ty}^2}, \tag{32}$$

which takes into account a few hundred Mev shift in the κ_{Tx} distribution due to the trigger bias. This yields

$$\frac{d\sigma^{\mathrm{smeared}}}{dz} = \int d\kappa_T \frac{dN}{d\kappa_T}\frac{d\sigma^{\mathrm{BORN}}}{dz} \sim \sqrt{\frac{A}{\pi}} e^{-p_T^2 A(1 - z - \bar{\kappa}/p_T)^2} \tag{33}$$

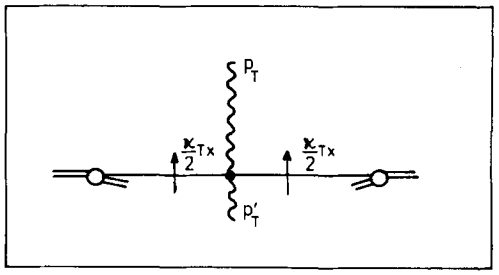

Fig. 11. Primordial parton $\langle \kappa_T \rangle$

Therefore the smeared Born term has a gaussian z-distribution which peaks at $\bar{z} = 1 - \bar{\kappa}/p_T$ with a width at half-maximum

$$\delta_z = 2.36/\sqrt{2Ap_T^2}. \tag{34}$$

For $\langle \kappa_T^2 \rangle = 1/A = .5$ GeV^2/c^2 [23] and $p_T = 4$ GeV/c, we get $\delta z = 0.3$ which is of the order of the perturbative width of Fig. 7. Notice that δz decreases as $1/p_T$, which implies that the primordial κ_T effect is completely hidden at large p_T by the perturbative effect.

It is now clear that for a large binning with $\Delta z \gg \delta z$, the effect of the smearing is negligible and the observed differential cross-section $d\sigma(\Delta z)/d\mathbf{p}_T dy dz$ can be directly compared to the perturbative calculation. On the other hand, to observe the primordial κ_T, we need a situation such that $W_p \ll \delta z$, where W_p is the width of the perturbative peak at half maximum; then the width of the observed peak of $d\sigma(\Delta z)/d\mathbf{p}_T\, dy\, dz$ around $z = 1$ will mainly be due to the smearing. It seems however that the condition $W_p \ll \delta z$ is difficult to realize. Let us for instance consider the case with $p_T = 4$ GeV/c and a small binning of $\Delta z = 0.08$, in order to get a good resolution of the perturbative peak (Fig. 12), still remaining in the validity domain of the $O(\alpha_s)$ calculation. This latter has a width $W_p \simeq 0.2$ which is not small compared to the non-perturbative width $\delta z \simeq 0.3$. It is therefore difficult to disentangle the perturbative from the non-perturbative effect.

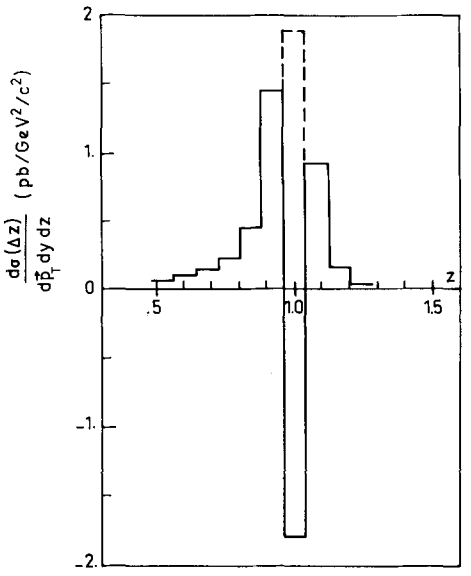

Fig. 12. Same as Fig. 7 but with $\Delta z = 0.08$

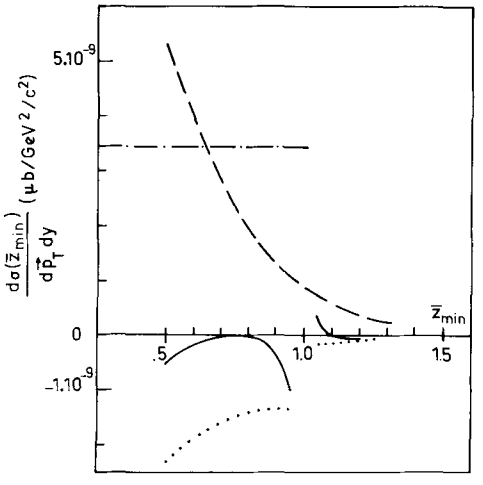

Fig. 13. $d\sigma(\bar{z}_{min})/d\mathbf{p}_T dy$ is a function of $\bar{z}_{min}$ for $pp \to \gamma\gamma X$ at $p_T = 8$ GeV/c, $y = 0$, $\sqrt{S} = 63$ GeV. The full (dotted) curve is the total ($gq \to \gamma\gamma q$) BLL contribution; the dash-dotted (dashed) curve is the Born (LL) contbibution

2. $pp \to \gamma\gamma X$ at $\sqrt{s} = 63$ GeV

Turning now to pp scattering at ISR energy, we expect a structure of the corrections quite different from the $\pi^- p$ case, because the relative importance of the quark-gluon initiated subprocesses is increased compared to the quark-antiquark one. We indeed verify, in Fig. 13, that the $qg \to \gamma\gamma q$ correction has almost the same absolute value as the $q\bar{q} \to \gamma\gamma g$ correction, but with opposite sign. As a result, the total BLL correction is small. The LL terms are no more negligible and give an important contribution to the low z part of the differential spectrum (Fig. 14). In that figure, it is the total differential spectrum (Born + Box + LL + BLL) which is shown.

With respect to the observation of the primordial κ_T, the situation is similar to that of the $\pi^- p \to \gamma\gamma x$ reaction: the perturbative width is of the order of the non-perturbative one.

3. $p\bar{p} \to \gamma\gamma X$ at $\sqrt{s} = 540$ GeV

At the collider energy and at $p_T = 30$ GeV/c, the predicted pattern of the corrections (Fig. 15) is similar to the one observed at SPS energy and $p_T = 4$ GeV/c for $\pi^- p \to \gamma\gamma X$. The cross-sections are however very small, because of the large value of p_T.

It can be seen in Fig. 16 (where the Box and LL contributions are not included) that the perturbative width is rather large ($W_p \simeq 0.17$) compared to the non-perturbative one ($\delta z \simeq 0.04$). Therefore the observation

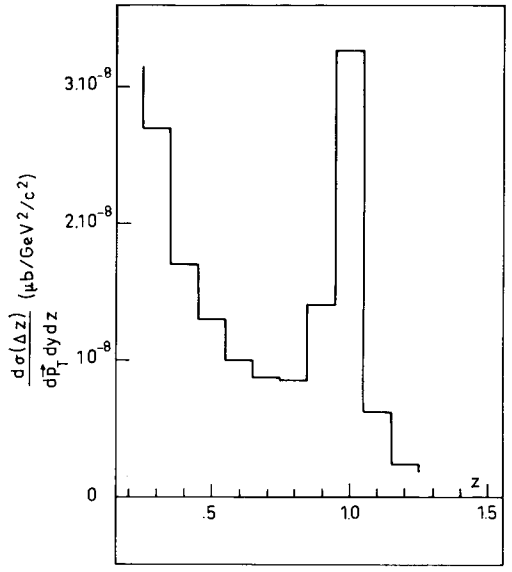

Fig. 14. $d\sigma(\Delta z)/d\mathbf{p}_T dydz$ as a function of z for $pp \to \gamma\gamma X$, at $p_T = 8$ GeV/c, $y = 0$, $\sqrt{S} = 63$ GeV with bins $\Delta z = 0.1$; total (Born + Box + LL + BLL) spectrum

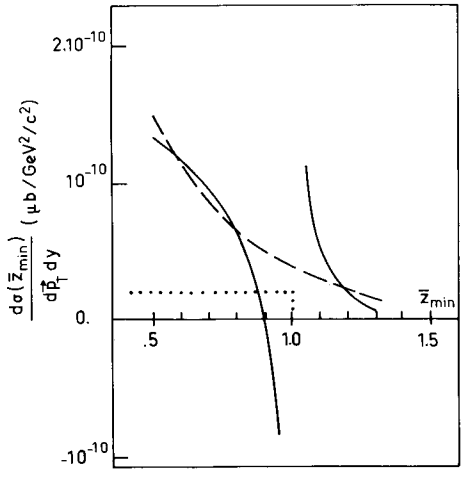

Fig. 15. $d\sigma(\bar{z}_{\min})/d\mathbf{p}_T dy$ as a function $\bar{z}_{\min}$ for $p\bar{p} \to \gamma\gamma X$ at $p_T = 30$ GeV/c, $y = 0$, $\sqrt{S} = 540$ GeV. The full (dashed) curve is the BLL (LL) contribution. The dotted curve is the box-diagram contributions

of $d\sigma(\Delta z)/d\mathbf{p}_T dydz$ would be a clear test of the BLL corrections.

4. Sensitivity with Respect to the Scale Q^2

Let us conclude this section by a discussion on the arbitrariness in the choice of the scale Q^2 which appears in the structure and fragmentation functions. At the LL level, this choice is arbitrary and some popular choices are $Q^2 = p_T^2$, $\hat{s}$, $2\hat{s}\hat{t}\hat{u}/(\hat{s}^2 + \hat{t}^2 + \hat{u}^2)$. Once the BLL corrections are included, this choice is still arbitrary, but there is now a compensation between the Born + LL terms and the BLL terms. To

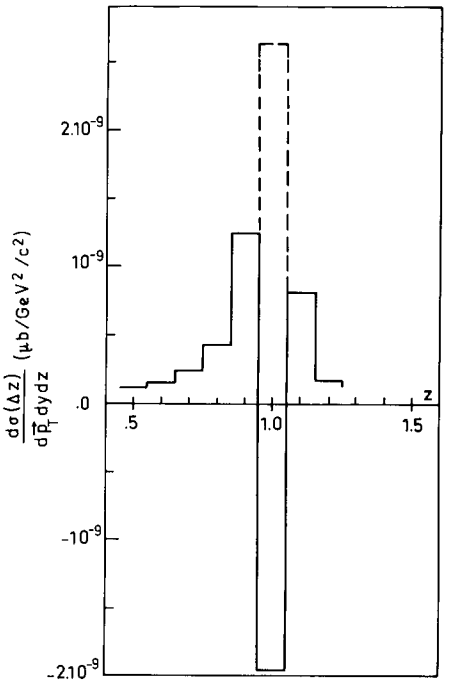

Fig. 16. $d\sigma(\Delta z)/d\mathbf{p}_T dydz$ for $p\bar{p} \to \gamma\gamma X$, $p_T = 30$ GeV/c, $y = 0$, $\sqrt{S} = 540$ GeV. Same conventions as Fig. 7. (Box and LL contributions are not shown)

demonstrate this compensation, let us study the differential spectrum of the $\pi^- p \to \gamma\gamma X$ reaction $d\sigma(\Delta z = .1)/d\mathbf{p}_T dydz$ in the bin around $z = 1.(p_T = 4$ GeV/c and $E = 300$ GeV). Choosing the scale $Q^2 = Cp_T^2$ and varying C between 0.5 and 16. (Notice that we keep $Q_c^2 = p_T^2$ fixed in the coupling constant $\alpha_s(Q_c^2)$), we find the Born contribution decreases by 40%, the BLL contribution changes from $-1.46 \cdot 10^{-6}$ μb/GeV^2/c^2 to $0.50 \cdot 10^{-6}$ μb/GeV/c^2 whereas the total cross-section varies by 25%.

IV. The P_{out} Distribution

When discussing higher order QCD contributions to $h_1 h_2 \to \gamma_1 \gamma_2 X$ one is naturally led to predict hadronic jets in the final state in addition to the two photons, and therefore non-coplanar two-photon events should be observed. The dominant subprocesses responsible for this are $q\bar{q} \to \gamma\gamma g$ (Fig. 3a) and $qg \to \gamma\gamma q$ (Fig. 3b). Consequently the expected rates are of order α_s.

In more detail, we present results for the aplanarity distribution to be measured in terms of p_{out}, which is the momentum of the photon γ_2 perpendicular to the plane defined by the trigger photon γ_1 and the incident hadron. Since the photons should be in opposite hemispheres we require as before a cut on $z = -\mathbf{p}_{T_1} \cdot \mathbf{p}_{T_2}/\mathbf{p}_{T_1}^2 \geqq \bar{z}_{\min}$. For p_{out} different from zero, the differential cross-section is then expressed in terms of the inelastic squared matrix elements $|M(q\bar{q} \to \gamma\gamma g)|^2$ and $|M(qg \to \gamma\gamma q)|^2$ described in Sect. II (but here

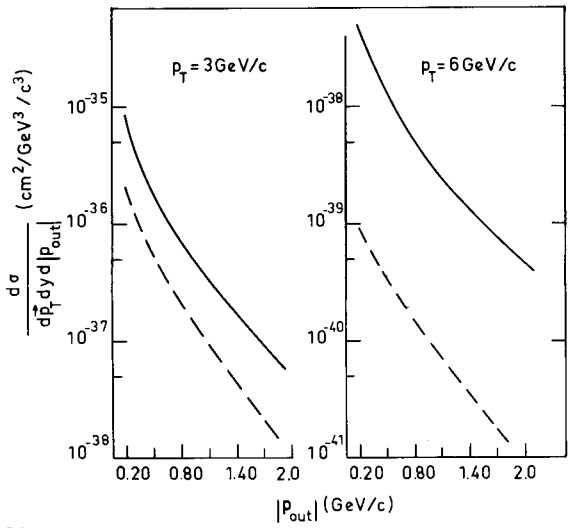

Fig. 17. $d\sigma/d\mathbf{p}_T dy d|p_{out}|$ for $\pi^- p \to \gamma\gamma X$ (full curve) and $pp \to \gamma\gamma X$ (dashed curve) as a function of $|p_{out}|$; $E_{Lab} = 300$ GeV, $y = 0$, $p_T = 3, 6$ GeV/c and $\bar{z}_{min} = 0.5$

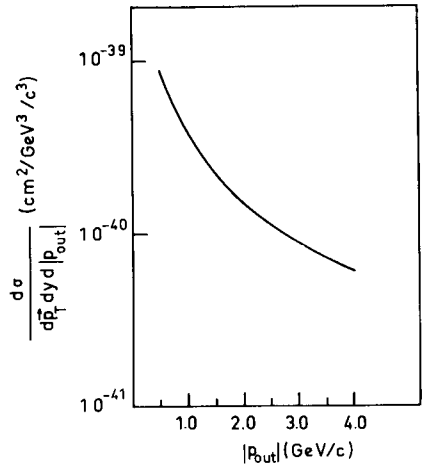

Fig. 18. $d\sigma/d\mathbf{p}_T dy d|p_{out}|$ for $p\bar{p} \to \gamma\gamma X$ as a function of $|p_{out}|$, $\sqrt{S} = 630$ GeV, $p_T = 30$ GeV/c, $y = 0$ and $\bar{z}_{min} = 0.5$

evaluated for $\varepsilon = 0$):

$$\frac{d\sigma(h_1 h_2 \to \gamma_1\gamma_2 X)}{d\mathbf{p}_T dy d|p_{out}|} = 2\int \frac{dx_1 dx_2}{\hat{s}} \int dy' \int_{\bar{z}_{min}} dz\,\theta(k_0)\delta(k^2) \cdot \sum_{a,b=q,g} G_{a/h_1}(x_1, Q^2) G_{b/h_2}(x_2, Q^2) \frac{p_T}{(4\pi)^5} |M(a+b \to \gamma_1(\mathbf{p}_T, y) + \gamma_2(p_{Tx} = -zp_T, p_{out}, y') + c(k))|^2. \quad (35)$$

Resulting p_{out} distributions, are shown in Fig. 17 and 18. These distributions diverge when $|p_{out}| = 0$ and would need some regularization procedure. We thus expect our results not to be reliable for too small $|p_{out}|$. At SPS energies the reactions $\pi^- p \to \gamma\gamma x$ and $pp \to \gamma\gamma x$ are compared at two values of the trigger p_T, $p_T = 3$ and 6 GeV/c, and $\bar{z}_{min} = 0.5$ (Fig. 17): the shape of the p_{out} dependence is the same, but the magnitudes of the cross-sections differ considerably, since $\pi^- p$ is dominated by $q\bar{q} \to \gamma\gamma g$, whereas $pp \to \gamma\gamma x$ by $qg \to \gamma\gamma q$. In both cases we find an average value $\langle |p_{out}| \rangle \simeq 0.5$ GeV/c (for $|p_{out}| \geqq 0.2$ GeV/c).

When increasing the energy, and the p_T of the trigger photon, the p_{out} distribution becomes broader. An example is given in Fig. 18 for $p\bar{p} \to \gamma\gamma X$ at SpS$\bar{p}$S and $p_T = 30$ GeV/c. The corresponding average is $\langle |p_{out}| \rangle \simeq 1.5$ GeV/c, for $|p_{out}| \geqq 0.5$ GeV/c.

IV. Conclusion

We have presented a complete calculation of the large p_T double photon production in hadronic collisions. The emphasis is put on $O(\alpha_s)$ corrections which turn out to be more important than the leading logarithm contributions associated to bremsstrahlung photons.

We choose to calculate z distributions $d\sigma/d\mathbf{p}_T dy dz$ $(h_1 h_2 \to \gamma_1\gamma_2 X)$ $(z = -\mathbf{p}_{T_1} \cdot \mathbf{p}_{T_2}/p_{T_1}^2)$, which show specific pattern for the various contributions: Born, leading logarithm and beyond leading logarithm contributions. Roughly speaking, the BLL correction widens the peak associated with the Born term $q\bar{q} \to \gamma\gamma$ and decreases its height. We discuss, in detail, the structure of the corrections, showing in particular that, to order α_s, one is led to define smeared distributions with resolution Δz or integrated distributions for z larger than a minimum experimental cut. In this last case, the ratio BLL/Born may be quite large—of the order of 50% in $\pi^- p$ collisions.

We give a rapid discussion of the primordial parton momentum $\langle \kappa_T \rangle$, showing that the hope to measure it from the lack of p_T balance of the 2 photons is destroyed by the importance of the perturbative corrections. This discussion should, however, be supplemented, in order to compare theory to data, by a detailed calculation of the smearing effect due to $\langle \kappa_T \rangle$. This would in particular tell us the magnitude of the associated "enhancement factor" for the observed distributions; with the now conventional value $\langle \kappa_T^2 \rangle \simeq 0.5$ (GeV/c)^2, this, even at relatively low $p_T \sim 2$ GeV/c, should not be larger than 2, decreasing rapidly with p_T. In the range of p_T where it is safe to neglect $\langle \kappa_T \rangle$, the measure of z distributions would provide a very interesting test of QCD (quark charges, value of α_s...). Finally, we also calculated aplanarity distributions characteristic of $O(\alpha_s)$ 3 jet configurations.

Appendix A

The cross-section for the subprocess $q + \bar{q} \to \gamma + \gamma$ is given in $4 - 2\varepsilon$ dimensions by

$$\frac{d\sigma^{q+\bar{q}\to\gamma+\gamma}}{dv}(\hat{s}, v) = \frac{1}{N_C} \alpha^2 e_q^4 F(\hat{s}, v, \varepsilon) T_0, \quad (A.1)$$

where $v = 1 + \hat{t}/\hat{s}$

with

$$F(\hat{s},v,\varepsilon)=\frac{2\pi}{\hat{s}}\mu^{2\varepsilon}\frac{1}{\Gamma(1-\varepsilon)}\left(\frac{4\pi\mu^2}{\hat{s}v(1-v)}\right)^{\varepsilon}, \tag{A.2}$$

and

$$T_0=(1-\varepsilon)\left((1-\varepsilon)\left(\frac{1-v}{v}+\frac{v}{1-v}\right)-2\varepsilon\right). \tag{A.3}$$

For $q+\bar{q}\to\gamma+g$, the cross-section is written as:

$$\frac{d\sigma^{q+q\to\gamma+g}}{dv}(\hat{s},v)=\frac{C_F}{N_C}\alpha\alpha_s e_q^2 F(\hat{s},v,\varepsilon)T_0. \tag{A.4}$$

For $q+g\to q+\gamma$, let us define as usual $\hat{t}=(p_g-p_\gamma)^2$, then

$$\frac{d\sigma^{q+g\to q+\gamma}}{dv}(\hat{s},v)=\frac{C_F}{N_C^2-1}\alpha\alpha_s e_q^2 F(\hat{s},v,\varepsilon)T'_0, \tag{A.5}$$

with

$$T'_0=(1-\varepsilon)\left((1-\varepsilon)\frac{1+v^2}{v}+2\varepsilon\right). \tag{A.6}$$

Let us now indicate how (26) is obtained. We start from (34) of [7] which we write under a convenient form for crossing as:

$$\frac{d\sigma^{\gamma+q\to\gamma+q}}{dv}(\hat{s},v)=\frac{\alpha_s}{2\pi}C_F\frac{\Gamma(1-\varepsilon)}{\Gamma(1-2\varepsilon)}\alpha^2 e_q^4 \cdot F(\hat{s},v,\varepsilon)\,\mathrm{Re}\,(\mathscr{A}(\hat{s},\hat{t},\hat{u})) \tag{A.7}$$

where $\mathscr{A}$ is a real analytic function given by:

$$\begin{aligned}\mathscr{A}(\hat{s},\hat{t},\hat{u})&=\left(\frac{4\pi\mu^2}{-\hat{s}}\right)^{\varepsilon}\left[\frac{\hat{s}+\hat{u}^2}{-\hat{s}\hat{u}}\left(-\frac{2}{\varepsilon^2}+\frac{1}{\varepsilon}\left(1-2\ln\frac{\hat{s}}{\hat{t}}\right)\right)-\frac{4}{\varepsilon}\right]\\&+\frac{\hat{s}^2+\hat{u}^2}{-\hat{s}\hat{u}}\left(\frac{5\pi^2}{3}-3+\ln^2\frac{\hat{t}}{\hat{u}}+4\ln\frac{\hat{s}}{\hat{t}}\right)\\&-\pi^2\left(2+\frac{\hat{u}}{\hat{s}}\right)-2-3\frac{\hat{s}}{\hat{u}}\ln\frac{\hat{u}}{\hat{s}}-6\ln\frac{\hat{s}}{\hat{t}}-2\ln\frac{\hat{u}}{\hat{t}}\\&-\left(2+\frac{\hat{u}}{\hat{s}}\right)\ln^2\frac{\hat{t}}{\hat{u}}-\left(2+\frac{\hat{s}}{\hat{u}}\right)\left(\ln^2\frac{\hat{t}}{\hat{s}}+\pi^2\right).\end{aligned} \tag{A.8}$$

We may now write, performing the crossing $\hat{s}\leftrightarrow\hat{t}$ (with an overall minus sign since crossing a fermion line:

$$\frac{d\sigma^{\text{virtual}}}{dv}(\hat{s},v)=\frac{\alpha_s}{2\pi}\frac{C_F}{N_C}\frac{\Gamma(1-\varepsilon)}{\Gamma(1-2\varepsilon)}\alpha^2 e_q^4 \cdot F(\hat{s},v,\varepsilon)\,\mathrm{Re}[-\mathscr{A}(\hat{t},\hat{s},\hat{u})]. \tag{A.9}$$

yielding (26).

Appendix B

The reader will be often referred to Appendix C of [7], which works out the method for calculations which are dealt with here.

1. Technical Points Related to the Calculation of $k(\hat{s},v,w,z)$

The constrained 3-particle phase-space (v, w and z are fixed) is written, in n dimensions:

$$\begin{aligned}(\mathrm{CPS})_3=\int&\frac{d^nk_1}{(2\pi)^{n-1}}\frac{d^nk_2}{(2\pi)^{n-1}}\frac{d^nk_3}{(2\pi)^{n-1}}\\&\cdot(2\pi)^n\delta^n(p+p'-k_1-k_2-k_3)\\&\cdot\delta^+(k_1^2)\delta^+(k_2^2)\delta^+(k_3^2)\delta\left(v-1-\frac{\hat{t}}{\hat{s}}\right)\\&\cdot\delta\left(w+\frac{\hat{u}}{\hat{s}+\hat{t}}\right)\delta(z-m\cdot k_2).\end{aligned} \tag{B.1}$$

It is calculated by going to the rest frame of k_2+k_3 in which we choose p, p', k_1 in such a way that they lie in the plane of the n^{th} and $n-1^{\text{th}}$ components of the momentum. Thus:

$$\begin{aligned}k_2&=\frac{\sqrt{s_2}}{2}(1,\ldots,\cos\theta_2\sin\theta_1,\cos\theta_1)\\k_3&=\frac{\sqrt{s_2}}{2}(1,\ldots,-\cos\theta_2\sin\theta_1,-\cos\theta_1),\end{aligned} \tag{B.2}$$

with $s_2=(k_2+k_3)^2=\hat{s}v(1-w)$ and where the dots indicate $n-3$ unspecified momenta which can be integrated over. We chose the axis so that

$$m=\left(\frac{\hat{s}}{\hat{t}\hat{u}}\right)^{1/2}(\mathrm{sh}\,\chi,0,\ldots,0,\mathrm{ch}\,\chi) \tag{B.3}$$

$$\text{with th}\,\chi=\sqrt{\frac{w(1-v)}{1-vw}}.$$

$$\begin{aligned}p&=\frac{\hat{s}v}{2\sqrt{s_2}}(1,0,\ldots,0,\sin\psi,\cos\psi)\\k_1&=\frac{\hat{s}(1-v+vw)}{2\sqrt{s_2}}(1,0,\ldots,0,\sin\psi'',\cos\psi'')\\p'&=\frac{\hat{s}(1-vw)}{2\sqrt{s_2}}(1,0,\ldots,0,-\sin\psi,\cos\psi),\end{aligned} \tag{B.4}$$

$$\text{with}\ \cos\psi=\text{th}\ \chi,\ \sin\psi=\sqrt{\frac{1-w}{1-vw}},$$

$$\begin{aligned}\cos\psi''&=\frac{1+v-vw}{1-v+vw}\cos\psi,\\\sin\psi''&=-\frac{1-v-vw}{1-v+vw}\sin\psi.\end{aligned} \tag{B.5}$$

Formula (B.1) leads to:

$$\begin{aligned}(\mathrm{CPS})_3=&\frac{\pi\hat{s}}{8(2\pi)^5}\left(\frac{4\pi}{\hat{s}}\right)^{\varepsilon}\frac{v}{\Gamma(1-2\varepsilon)}\left(\frac{4\pi}{\hat{s}vw(1-v)}\right)^{\varepsilon}\\&\cdot v^{-\varepsilon}(1-w)^{-\varepsilon}\int_0^{\pi}d\theta_1\,d\theta_2(\sin\theta_1)^{1-2\varepsilon}\\&\cdot(\sin\theta_2)^{-2\varepsilon}\delta(z-m\cdot k_2)\end{aligned} \tag{B.6}$$

Integrating on θ_1 is trivial since $z=\frac{1}{2}(1-\cos\theta_1 \coth\chi)$ which also shows $z_{\min}^{\max}=\frac{1}{2}(1\pm\coth\chi)$. The result is:

$$(\mathrm{CPS})_3=\frac{\pi\hat{s}}{8(2\pi)^5}\left(\frac{4\pi}{\hat{s}}\right)^{\varepsilon}\frac{v}{\Gamma(1-2\varepsilon)}\left(\frac{4\pi}{\hat{s}vw(1-v)}\right)^{\varepsilon}\cdot c(v,w,z)\int_0^{\pi}d\theta_2(\sin\theta_2)^{-2\varepsilon} \tag{B.7}$$

with

$$c(v,w,z)=v^{-\varepsilon}(1-w)^{-\varepsilon}2\sqrt{\frac{w(1-v)}{1-vw}}\cdot\left[\frac{1-w+4w(1-v)z(1-z)}{1-vw}\right]^{-\varepsilon} \tag{B.8}$$

Let us now discuss the integrals which appear when integrating $|M|^2$ over θ_2. For simplicity, we define the quantity

$$\mathscr{J}=c(v,w,z)\int_0^{\pi}d\theta_2(\sin\theta_2)^{-2\varepsilon}|M|^2 \tag{B.9}$$

which can be expressed in terms of standard integrals to be classified in 3 types:

(*i*) *Non singular integrals* ($z>0$) which may be straightforwardly calculated, using, for instance, the method developed in [7, Appendix C (C.12)]. One example is the integral

$$JA_2=c(v,w,z)\int_0^{\pi}d\theta_2(\sin\theta_2)^{-2\varepsilon}\frac{1}{a_2}=\frac{4\pi}{\hat{s}v}\frac{1}{z}. \tag{B.10}$$

(*ii*) *Singular integrals in the variable z only, at* $z=1$. Similarly to the case treated in [7, Appendix C (C.14)], the integral

$$JA_3=c(v,w,z)\int_0^{\pi}d\theta_2(\sin\theta_2)^{-2\varepsilon}\frac{1}{a_3}, \tag{B.11}$$

is expressed in terms of singular distributions:

$$JA_3=\frac{4\pi}{\hat{s}v}v^{-\varepsilon}(1-w)^{-\varepsilon}\left[\left(-\frac{1}{\varepsilon}-\ln z_{\max}\right)\delta(1-z)+\frac{\theta(1-z)}{(1-z)_+}+\frac{\theta(z-1)}{(z-1)_+}\right], \tag{B.12}$$

where $1/(z-1)_+$ is defined by

$$\int_1^{z_{\max}}\frac{f(z)}{(z-1)_+}=\int_1^{z_{\max}}\frac{f(z)-f(1)}{z-1}. \tag{B.13}$$

(*iii*) *Singular integrals in both variables z and w* Let us treat in detail the case of

$$I_{33}=c(v,w,z)\int_0^{\pi}d\theta_2(\sin\theta_2)^{-2\varepsilon}\frac{1}{a_3b_3}, \tag{B.14}$$

which takes the form:

$$I_{33}=\frac{4}{\hat{s}v}\frac{4}{\hat{s}(1-vw)}c(v,w,z)\frac{2^{2\varepsilon}}{1+\cos\theta_1\cos\psi}I(a,b), \tag{B.15}$$

with $\cos\theta_1=\mathrm{th}\,\chi\,(1-2z)$ and

$$I(a,b)=2^{-2\varepsilon}\int_0^{\pi}d\theta_2\frac{(\sin\theta_2)^{-2\varepsilon}}{1+a+b\cos\theta_2}, \tag{B.16}$$

where $a=\cos\theta_1\cos\psi$, $b=\sin\theta_1\sin\psi$. Defining $a'=\sin\psi/2\,\sin\theta_1/2$ and $b'=\cos\psi/2\,\cos\theta_1/2$ with $b'^2-a'^2=(1-z)\mathrm{th}\,\chi$, we may write $I(a,b)$ under the symmetric form:

$$I(a,b)=\frac{\pi I_0}{2}\frac{(a'^2+b'^2)^{2\varepsilon}}{|a'^2-b'^2|^{1+2\varepsilon}}\cdot F\left(\frac{1}{2}-\varepsilon,-\varepsilon,1-\varepsilon;\frac{4a'^2b'^2}{(a'^2+b'^2)^2}\right), \tag{B.17}$$

where $I_0=\Gamma(1-2\varepsilon)/\Gamma^2(1-\varepsilon)=1+\varepsilon^2\,(\pi^2/6)+O(\varepsilon^3)$ and F is the usual hypergeometric function [24]. So that I_{33} may be finally written under the form:

$$I_{33}=\frac{4}{\hat{s}v}\frac{4}{\hat{s}(1-vw)}v^{-\varepsilon}\pi I_0\left(\frac{1}{1-w}\right)^{1+\varepsilon}\cdot\left|\frac{1}{1-z}\right|^{1+2\varepsilon}g(v,w,z)\cdot F(\tfrac{1}{2}-\varepsilon,-\varepsilon,1-\varepsilon;h(v,w,z)), \tag{B.18}$$

with

$$g(v,w,z)=(w(1-v))^{-\varepsilon}\cdot[1-w+4w(1-v)z(1-z)]^{-\varepsilon}\cdot[1-w+2w(1-v)(1-z)]^{2\varepsilon}\cdot\frac{(1-vw)(1-w)}{(1-w)+2(1-z)w(1-v)}, \tag{B.19}$$

and where the argument $h(v,w,z)$ of the hypergeometric function is equal to 0 when w goes to 1 in which case $F(\frac{1}{2}-\varepsilon,-\varepsilon,1-\varepsilon;0)=1$ and equal to 1 when z goes to 1 with $F(\frac{1}{2}-\varepsilon,-\varepsilon,1-\varepsilon;1)=2^{-\varepsilon}(1+O(\varepsilon^2))$.

In order to express I_{33} in terms of usual distributions, we define it by its action on a test function $f(w,z)$ introducing

$$\mathscr{I}_{33}=\frac{\hat{s}v}{4}\frac{\hat{s}(1-vw)}{4}v^{\varepsilon}\int dwdz\,I_{33}f(w,z), \tag{B.20}$$

which may be cast out into

$$\mathscr{I}_{33}=I_1+I_2 \tag{B.21}$$

with

$$I_1=\frac{\hat{s}v}{4}\frac{\hat{s}(1-vw)}{4}v^{\varepsilon}\int dwdz\,I_{33}(f(w,z)-f(w,1)), \tag{B.22}$$

and

$$I_2=\frac{\hat{s}v}{4}\frac{\hat{s}(1-vw)}{4}v^{\varepsilon}\int dwdz\,I_{33}f(w,1). \tag{B.23}$$

The first integral is treated straightforwardly and we are led to study I_2 which may be written as:

$$I_2=\int_0^1\frac{dw}{(1-w)^{1+\varepsilon}}f(w,1)\int_0^{z_{\max}}dz\frac{\pi I_0 g(v,w,z)F}{|1-z|^{1+2\varepsilon}}. \tag{B.24}$$

Using [7]

$$\int_0^\pi d\theta_1 d\theta_2 (\sin\theta_1)^{1-2\varepsilon}(\sin\theta_2)^{-2\varepsilon}\frac{1}{a_3 b_3}$$
$$=\frac{4}{\hat{s}v}\frac{4}{\hat{s}(1-vw)}\int_{z_{\min}}^{z_{\max}}\frac{\pi I_0 g F}{(1-w)|1-z|^{1+2\varepsilon}}$$
$$=\frac{4}{\hat{s}v}\frac{4}{\hat{s}(1-vw)}\left\{-\frac{\pi}{\varepsilon}\left(\sin^2\frac{\varphi}{2}\right)^{-1-\varepsilon}\right.$$
$$\left.\cdot\left(1+\varepsilon^2\,\mathrm{Li}_2\left(\cos^2\frac{\varphi}{2}\right)+O(\varepsilon^3)\right)\right\}, \tag{B.25}$$

with $\sin^2\varphi/2=(1-w)/(1-vw)$, we get

$$\int_0^{z_{\max}} dz\frac{\pi I_0 g F}{|1-z|^{1+2\varepsilon}}=-\frac{\pi}{\varepsilon}(1-vw)$$
$$\cdot\left(\frac{1-w}{1-vw}\right)^{-\varepsilon}\left(1+\varepsilon^2\,\mathrm{Li}_2\left(\cos^2\frac{\varphi}{2}\right)+O(\varepsilon^3)\right)$$
$$-\pi I_0\int_{z_{\min}}^{0} dz\frac{1}{1-z}\frac{(1-vw)(1-w)}{D_1}+O(\varepsilon(1-w)), \tag{B.26}$$

with $D_1=1-w+2(1-z)w(1-v)$. After some algebra, the final result is:

$$I_{33}=\frac{16\pi}{\hat{s}^2 v(1-vw)}v^{-\varepsilon}I_0\left\{(1-vw)\left[\frac{\theta(1-z)}{(D_1(1-z))_+}\right.\right.$$
$$\left.+\frac{\theta(z-1)}{(D_1(z-1))_+}\right]+\delta(1-z)\left[-\frac{1-vw}{1-w}\ln\frac{\mathrm{th}\,\chi+\coth\chi}{2}\right.$$
$$+v\left(-\frac{1}{\varepsilon}-\ln(1-vw)+2\ln(1-w)\right)$$
$$-(1-v)\left(\left(\frac{1}{\varepsilon}+\ln(1-v)\right)\left(\frac{1}{1-w}\right)_+\right.$$
$$\left.\left.-2\left(\frac{\ln(1-w)}{1-w}\right)_+ +\frac{\ln((1-vw)/(1-v))}{1-w}\right)\right]$$
$$+\delta(1-z)\delta(1-w)\left[\frac{1}{2\varepsilon^2}+\frac{1}{2\varepsilon}\ln(1-v)\right.$$
$$\left.\left.+\tfrac{1}{4}\ln^2(1-v)\right](1-v)\right\}, \tag{B.27}$$

where $1/(D_1(1-z))_+$ is defined by

$$\int_0^1 dz\frac{f(z)}{(D_1(1-z))_+}=\int_0^1 dz\frac{f(z)-f(1)}{D_1(1-z)}$$

and $1/(D_1(z-1))_+$ analogously:

$$\int_1^{z_{\max}} dz\frac{f(z)}{(D_1(z-1))_+}=\int_1^{z_{\max}} dz\frac{f(z)-f(1)}{D_1(z-1)}.$$

2. Calculation of $k'(\hat{s},v,w,z)$

We now turn to the calculation of integrals corresponding to $g+q\to\gamma+\gamma+q$. We shall adopt the same labels and conventions for the momenta than in Appendix C of [7], so that the subprocess $g(k_1)+q(p)\to\gamma(k_2)+\gamma(k_3)+q(p')$ is described by the same matrix element as in [7] (up to a colour factor). We have

$$p=\hat{s}(1-vw)/2\sqrt{s_2}\quad(1,0,\ldots,0,\sin\psi,\cos\psi)$$
$$k_1=\hat{s}v/2\sqrt{s_2}\quad(1,0,\ldots,0,-\sin\psi,\cos\psi) \tag{B.28}$$
$$k_2=\hat{s}(1-v+vw)/2\sqrt{s_2}\quad(1,0,\ldots,0,\sin\psi'',\cos\psi''),$$

and

$$p'=\sqrt{s_2}/2\quad(1,\ldots,\cos\theta_2\sin\theta_1,\cos\theta_1)$$
$$k_3=\sqrt{s_2}/2\quad(1,\ldots,-\cos\theta_2\sin\theta_1,-\cos\theta_1). \tag{B.29}$$

In the present case, where we observe the 2 photons, (as opposed to photon-quark in [7]) the variable z is defined by

$$z=m\cdot k_3=1-m\cdot p'=\frac{1+\cos\theta_1\coth\chi}{2}, \tag{B.30}$$

where $m=(\hat{s}/\hat{t}\hat{u})^{1/2}$ (sh χ, 0,...,0, ch χ)

The constrained phase-space takes the same form as in (B.7). The collinear singularities, encountered when integrating on θ_2, corresponding to b_1, $b_2=0$ correspond to singularities in z: $z=1$ and $z=z_1=1/(1-v+vw)$ respectively. As above, let us consider integrals with various singular behaviours:

i) Integrals which involve singularities at $z=1$ are treated in the standard way. For instance

$$\overline{JB_1}=c(v,w,z)\int_0^\pi d\theta_2(\sin\theta_2)^{-\varepsilon}\frac{1}{b_1}, \tag{B.31}$$

is trivially seen to be equal to JA_3 (given by (B.12))

ii) Let us examine integrals which involve singularities at $z=z_1$. An example is

$$\overline{JB_2}=c(v,w,z)\int_0^\pi d\theta_2(\sin\theta_2)^{-\varepsilon}\frac{1}{b_2}, \tag{B.32}$$

which may be written:

$$\overline{JB_2}=\frac{4}{\hat{s}(1-v+vw)}c(v,w,z)\,2^{2\varepsilon}I(\bar{a},\bar{b}), \tag{B.33}$$

with

$$I(\bar{a},\bar{b})=2^{-2\varepsilon}\int_0^\pi d\theta_2\frac{(\sin\theta_2)^{-2\varepsilon}}{1-\bar{a}-\bar{b}\cos\theta_2}, \tag{B.34}$$

where $\bar{a}=\cos\theta_1\cos\psi'',\bar{b}=\sin\theta_1\sin\psi''$. Introducing $\bar{a}'=\sin\psi''/2\quad\cos\theta_1/2$ and $\bar{b}'=\cos\psi''/2\sin\theta_1/2$ with $b'^2-a'^2=(z_1-z)\mathrm{th}\,\chi$, we find

$$I(\bar{a},\bar{b})=\pi\frac{I_0}{2}\frac{(\bar{a}'^2+b''^2)^{2\varepsilon}}{|\bar{a}'^2-\bar{b}'^2|^{1+2\varepsilon}}$$
$$\cdot F\left(\frac{1}{2}-\varepsilon,-\varepsilon,1-\varepsilon;\frac{4\bar{a}'^2\bar{b}'^2}{(\bar{a}'^2+\bar{b}'^2)^2}\right), \tag{B.35}$$

so that

$$\overline{JB_2}=\frac{4}{\hat{s}(1-v+vw)}\pi I_0 v^{-\varepsilon}(1-w)^{-\varepsilon}\bar{g}(v,w,z)$$
$$\cdot\frac{1}{|z_1-z|^{1+2\varepsilon}}F(\tfrac{1}{2}-\varepsilon,-\varepsilon,1-\varepsilon;\bar{h}(v,w,z)), \tag{B.36}$$

where

$$\bar{g}(v,w,z)=(w(1-v))^{-\varepsilon}\{(1-w+4w(1-v)z(1-z))^{-\varepsilon}\cdot(1-w+2w(1-v)(1+v-vw)z_1(z_1-z)-4vw(1-v)(1-w)z_1^2)^{2\varepsilon}\}, \quad \text{(B.37)}$$

and the argument $\bar{h}$ of the hypergeometric functions goes to 1 when z is equal to z_1. Similarly to (B.12), we obtain $\overline{JB_2}$ in terms of the distributions $\delta(z-z_1)\cdots$:

$$\overline{JB_2}=\frac{4\pi}{\hat{s}(1-v+vw)}I_0 v^{-\varepsilon}(1-w)^{-\varepsilon}\cdot\left\{\delta(z-z_1)\left(-\frac{1}{\varepsilon}-\ln\left(1-\frac{z_{\min}}{z_1}\right)\right)+\left(\frac{1}{z_1-z}\right)_+\theta(z_1-z)+\left(\frac{1}{z-z_1}\right)_+\theta(z-z_1)\right\}. \quad \text{(B.38)}$$

iii) In order to calculate integrals such as

$$\overline{JB_2W}=c(v,w,z)\frac{1}{1-w}\int_0^\pi d\theta_2\frac{(\sin\theta_2)^{-2\varepsilon}}{b_2} \quad \text{(B.39)}$$

we have to deal with the same problem as above (B.18) of disentangling singularities in z and w. The integral $\overline{JB_2W}$ is written as:

$$\overline{JB_2W}=\frac{4\pi I_0}{\hat{s}(1-v+vw)}v^{-\varepsilon}\frac{1}{(1-w)^{1+\varepsilon}}\cdot\frac{1}{|z_1-z|^{1+2\varepsilon}}\bar{g}(v,w,z)\cdot F(\tfrac{1}{2}-\varepsilon,-\varepsilon,1-\varepsilon;\bar{h}(v,w,z)) \quad \text{(B.40)}$$

As in (B.23), we are led to calculate

$$I_3=\int_0^1\frac{dw}{(1-w)^{1+\varepsilon}}f(w,z_1)\int_0^{z_{\max}}\frac{\pi I_0\bar{g}(v,w,z)F}{|z_1-z|^{1+2\varepsilon}} \quad \text{(B.41)}$$

Using the same trick as in (B.25), we find:

$$\overline{JB_2W}=\frac{4\pi}{\hat{s}(1-v+vw)}I_0v^{-\varepsilon}\left\{-\frac{1}{\varepsilon}\delta(1-w)\cdot\left[\left(\frac{1}{1-z}\right)_+-\varepsilon\left(\frac{\ln(1-z)}{1-z}\right)_+-\varepsilon\frac{\ln z}{1-z}\right]\theta(1-z)+\left(\frac{1}{1-w}\right)_+\left[\frac{\theta(z_1-z)}{(z_1-z)_+}+\frac{\theta(z-z_1)}{(z-z_1)_+}\right]+\frac{1}{\varepsilon^2}\delta(1-w)\delta(1-z)+\delta(z_1-z)\left[-\frac{1}{\varepsilon}\left(\frac{1}{1-w}\right)_+\right.\right.+\left.\left.\left(\frac{\ln(1-w)}{1-w}\right)_+-\ln\left(1-\frac{z_{\min}}{z_1}\right)\frac{1}{1-w}\right]\right\}. \quad \text{(B.42)}$$

iv) A new situation, as compared to previous Sect. 1 of this appendix occurs when integrals have both singularities $z=1$ and $z=z_1$. This is the case for

$$\overline{I_{12}}=c(v,w,z)\int_0^\pi d\theta_2(\sin\theta_2)^{-2\varepsilon}\frac{1}{b_1b_2}$$

$$=\frac{1}{\hat{s}(1-v)}\frac{1}{1+w(1-2z)}\left\{\frac{1-v-vw}{v}\overline{JB_2}+\overline{JB_1}\right\}. \quad \text{(B.43)}$$

Using

$$\frac{1}{1+w(1-2z)}\left(\frac{1}{1-z}\right)_+=\frac{1}{1-w}\left(\frac{1}{1-z}\right)_+-\frac{1}{1-w}\frac{1}{\bar{z}-z}$$

$$\frac{1}{1+w(1-2z)}\left(\frac{1}{z-1}\right)_+=\frac{1}{1-w}\left(\frac{1}{z-1}\right)_++\frac{1}{1-w}\frac{1}{\bar{z}-z}$$

$$\frac{1}{1+w(1-2z)}\left(\frac{1}{z_1-z}\right)_+=\frac{1}{2w\bar{z}-z_1}\left(\frac{1}{z_1-z}\right)_+-\frac{1}{2w\bar{z}-z}\frac{1}{\bar{z}-z_1}$$

$$\frac{1}{1+w(1-2z)}\left(\frac{1}{z-z_1}\right)_+=\frac{1}{2w\bar{z}-z_1}\left(\frac{1}{z-z_1}\right)_++\frac{1}{2w\bar{z}-z}\frac{1}{\bar{z}-z_1}, \quad \text{(B.44)}$$

where $\bar{z}=(1+w)/2w$, we find

$$\bar{I}_{12}=\frac{8\pi}{\hat{s}^2}\frac{1}{v(1-v)}I_0v^{-\varepsilon}(1-w)^{-\varepsilon}\cdot\left\{\delta(z-z_1)\left[-\frac{1}{\varepsilon}-\ln\left(1-\frac{z_{\min}}{z_1}\right)\right]+\delta(z-1)\left[-\frac{1}{\varepsilon}-\ln z_{\max}\right]+\theta(1-z)\left[\frac{1}{(1-z)_+}-\frac{2}{\bar{z}-z}\right]+\left(\frac{1}{z-1}\right)_+\theta(z-1)+\left(\frac{1}{z_1-z}\right)_+\theta(z_1-z)+\left(\frac{1}{z-z_1}\right)_+\theta(z-z_1)+\frac{2}{\bar{z}-z}\theta(z-z_1)\right\}\frac{1}{1-w}. \quad \text{(B.45)}$$

Notice that in the calculation $\bar{I}_{12}$ appears always multiplied by $(1-w)$. The term $\theta(1-z)/\bar{z}-z$ is not singular since $\bar{z}>1$. On the other hand, for the term $\theta(z-z_1)/\bar{z}-z$, it should be remarked that, except when $w=1$, $\bar{z}$ is always lying in the interval $[1,z_1]$.

3. Integrating on z

As stated in Section II, we shall integrate the final result for $d\sigma/d\mathbf{p}_{T_1}dy_1dz$ over z in the interval $[\bar{z}_{\min},\bar{z}_{\max}]$ or bins Δz. We may perform this integration before integrating on v and w so that we shall deal with integrating in the interval $[z_{\min},z_{\max}(v,w)]$.

The distributions which appear in the calculation of k and k' are, however, defined in intervals $[0,1]$ or $[0,z_1]$ and $[1,z_{max}]$ or $[z_1,z_{max}]$. Let us first discuss the case when $\bar{z}_{min}<1$. It is convenient to define distributions in the interval $[\bar{z}_{min},1]$ or $[\bar{z}_{min},z_1]$ and make the following substitutions*:

$$\left(\frac{1}{1-z}\right)_+ = \left(\frac{1}{1-z}\right)_{\bar{z}_{min}} + \ln(1-\bar{z}_{min})\delta(1-z)$$

$$\left(\frac{1}{D_1(1-z)}\right)_+ = \left(\frac{1}{D_1(1-z)}\right)_{\bar{z}_{min}} + \frac{1}{1-w} \cdot\ln\left[\frac{(1-\bar{z}_{min})(2w(1-v)+(1-w))}{2w(1-\bar{z}_{min})(1-v)+1-w}\right] \cdot\delta(1-z),$$

where $1/(1-z)_{\bar{z}_{min}}$ is defined by

$$\int_{\bar{z}_{min}}^{1} dz \frac{f(z)}{(1-z)_{\bar{z}_{min}}} = \int_{\bar{z}_{min}}^{1} dz \frac{f(z)-f(1)}{1-z},$$

and $1/(D_1(1-z))_{\bar{z}_{min}}$ is similarly defined by

$$\int_{\bar{z}_{min}}^{1} dz \frac{f(z)}{(D_1(1-z))_{\bar{z}_{min}}} = \int_{\bar{z}_{min}}^{1} dz \frac{f(z)-f(1)}{D_1(1-z)}.$$

In the same fashion

$1/(z_1-z)_+$ should be replaced by:

$$\left(\frac{1}{z_1-z}\right)_+ = \left(\frac{1}{z_1-z}\right)_{\bar{z}_{min}} + \delta(z_1-z)\ln(z_1-\bar{z}_{min})$$

with $1/(z_1-z)_{\bar{z}_{min}}$ defined by

$$\int_{\bar{z}_{min}}^{z_1} dz \frac{f(z)}{(z_1-z)_{\bar{z}_{min}}} = \int_{\bar{z}_{min}}^{z_1} dz \frac{f(z)-f(z_1)}{z_1-z}.$$

If $\bar{z}_{min}>1$, integrals corresponding to expressions proportional to $\theta(1-z)$ go to 0. When *i)* $\bar{z}_{min}<z_1$, integrating between $\bar{z}_{min}$ and z_{max}, one should replace $(1/(z-1))_+$ by $1/(z-1)$ and $1/(D_1(z-1))_+$ by $1/D_1(z-1)$; when ii) $\bar{z}_{min}>z_1$, integrals corresponding to expressions proportional to $\theta(z_1-z)$ go to 0, and $1/(z-z_1)_+$ should be replaced by $1/(z-z_1)$.

References

1. T. Ferbel, W.R. Molzon: Rev. Mod. Phys. **56**, 181 (1984); see also N. Willis: Proceedings of the 4th International Colloquium on photon–photon interactions. Paris 1981 ed. G.W. London, Singapore: World Scientific 1981
2. E.L. Berger, E. Braaten, R.D. Field: Nucl. Phys. **B239**, 52 (1984) and references therein
3. S. Berman, J. Bjorken, J. Kogut: Phys. Rev. D4, **1418** (1971)
4. T. Jayaraman: Contribution to the VIth International Workshop on photon–photon collisions (Lake Tahoe, 1984) and references therein
5. B.L. Combridge: Nucl. Phys. **B174**, 243 (1980); C. Carimalo, M. Crozon, P. Kessler, J. Parisi: Phys. Lett. **98B**, 105 (1981)
6. C.H. Llewellyn Smith: Phys. Lett. **79B**, 83 (1978)
7. P. Aurenche et al.: Z. Phys. C—Particles and Fields **24**, 309 (1984)
8. C.J. Gilmour: preprint DAMTP 84/19
9. C.A. Garcia-Canal, J.A. Grifols, A. Mendez: Phys. Lett. **146B**, 244 (1984); A. Ali et al.: preprint CERN-TH.3959/84
10. A. Nicolaïdis: Nucl. Phys. **B163**, 156 (1980)
11. R.K. Ellis et al.: Nucl. Phys. **B152**, 285 (1979); D. Amati, R. Petronzio and G. Veneziano: Nucl. Phys. **B146**, 29 (1978)
12. R.K. Ellis, M.A. Furman, H.E. Haber I. Hinchliffe: Nucl. Phys. **B173**, 397 (1980)
13. G. Altarelli, G. Parisi: Nucl. Phys. **B126**, 298 (1977).
14. G. Altarelli, R.K. Ellis and G. Martinelli: Nucl. Phys. **B143**, 521 (1978)
15. G.'t Hooft, M. Veltman: Nucl. Phys. **B44**, 189 (1972); C.G. Bollini, J.J. Giambiagi: Nuovo Cimento **12B**, 20 (1972); W.J. Marciano: Phys. Rev. **D12**, 3861 (1975)
16. L. Baulieu, C. Kounnas: Nucl. Phys. **B141**, 423 (1978); L. Kodaira, T. Uematsu: Nucl. Phys. **B141**, 497 (1978)
17. R. Baier, J. Engels, B. Petersson: Z. Phys. C—Particles and Fields **2**, 265 (1979)
18. H. Abramovicz et al.: Z. Phys. C—Particles and Fields **12**, 289 (1982)
19. J.F. Owens: Phys. Rev. **D30**, 943 (1984)
20. J.C.H. de Groot et al.: Z. Phys. C—Particles and Fields **1**, 143 (1979)
21. A. Bassetto, M. Ciafaloni, G. Marchesini: Phys. Rep. **100**, 201 (1983)
22. G. Parisi, R. Petronzio: Nucl. Phys. **B154**, 427 (1979).
23. P. Chiappetta, M. Greco: Nucl. Phys. **B221**, 269 (1983).
24. A. Erdelyi, W. Magnus, F. Oberhettinger, F.G. Tricomi: Bateman manuscript. New York: McGraw-Hill 1953

* Similarly, when integrating on w, between a lower bound A and 1, one makes the substitutions $1/(1-w)_+ = 1/(1-w)_A + \delta(1-w)\ln(1-A)$ and $(\ln(1-w)/(1-w))_+ = (\ln(1-w)/(1-w))_A + \frac{1}{2}\ln^2(1-A)\delta(1-w)$